MICROSCOPIC AND GEOCHEMICAL STUDIES OF ANCIENT, POTENTIALLY RIFT-RELATED PLUTONIC IGNEOUS ROCKS IN COLORADO

By

Isabella Marina Niño

Submitted in partial fulfillment of the

requirements for Departmental Honors in

the Department of Geological Sciences

Texas Christian University

Fort Worth, Texas

December 9, 2024

MICROSCOPIC AND GEOCHEMICAL STUDIES OF ANCIENT, POTENTIALLY RIFT-RELATED PLUTONIC IGNEOUS ROCKS IN COLORADO

Project Approved:

Supervising Professor: Richard Hanson, Ph.D.

Department of Geological Sciences

Xiangyang Xie, Ph.D.

Department of Geological Sciences

Brendan Lavy, Ph.D.

Department of Environmental and Sustainability Sciences

Abstract

The regional geological framework of the area I am studying involves a possible major northwest-trending Cambrian to Ordovician rift zone with abundant igneous rocks in parts of Colorado. These igneous rocks may be related to large volumes of Cambrian igneous rocks located along the same trend in Southern Oklahoma and nearby parts of Texas within the large-scale Southern Oklahoma rift zone. My project focuses on plutonic igneous intrusions located in the Wet Mountains in the southern part of the Front Range in Colorado and the Powderhorn District farther west. This thesis reports the results of microscopic and geochemical studies carried out on three main intrusions in the Wet Mountains as well as important rock units within the Powderhorn District. Samples of gabbro and pyroxenite from the McClure Mountain Complex show evidence of the accumulation of crystals on the floor of the magma chamber. Trace element contents in younger nepheline-bearing syenites suggest these rocks were partly derived from more than one batch of magma injected into a single magma chamber. Nepheline syenites also present in the Powderhorn Complex have somewhat different geochemical contents from those in the McClure Mountain Complex indicating they are not directly related. A large body of carbonatite in the Powderhorn Complex formed by an intrusion of an entirely separate magma that was injected in pulses. The presence of nepheline syenites in the Colorado intrusions requires the production of silica-undersaturated magmas, which could not have been directly related to silica-oversaturated igneous rocks in the Southern Oklahoma rift zone. The Colorado intrusions may have formed in a continuation of the Southern Oklahoma rift zone but were produced by different igneous processes.

Introduction

Located in southern Oklahoma and nearby areas of Texas, a major Early Cambrian rift termed the Southern Oklahoma rift zone hosts a large igneous assemblage (Hanson et al., 2013; Wall et al., 2021). These rocks consist of extensive rhyolites (silicic volcanic rocks) as well as intrusive granites and other intrusive rock types, and are exposed in both the Wichita Mountains and the Arbuckle Mountains in southern Oklahoma (Fig. 1). They record one of the most significant magmatic events linked to the Cambrian opening of the Iapetus Ocean along the eastern or southern margins of Laurentia (the ancient core of North America) (Fig. 2). It is speculated that abundant Cambrian to Ordovician alkalic igneous rocks in parts of Colorado located along the same trend may be a continuation of the rift (Larson et al., 1985; Magnin et al., 2023) (Fig. 1). These rocks in Colorado consist of dikes (where magma intruded along fissures) and larger intrusive masses (plutons), which form when magma solidifies at deeper levels. The objective of this project is to investigate the mineralogical and geochemical characteristics of the plutonic intrusions along this trend in Colorado.

Cambrian and Ordovician Plutonic Rocks in Colorado

Cambrian and Ordovician alkalic plutonic rocks occur in two main locations in Colorado, in the Wet Mountains and the Powderhorn area farther west (Fig. 1.). In both areas, the plutons intrude older Proterozoic granites and metamorphic rocks (Olson et al., 1977). An alkalic igneous complex has been recognized in Colorado's Powderhorn district for nearly a century, with three main plutonic intrusions within the Wet Mountains being recognized more recently. These intrusions include the McClure Mountain Complex, Gem Park Complex, and Democrat Creek Complex (Fig. 3). Geological mapping in the Powderhorn District and the Wet Mountains has also identified numerous dikes that are thought to be tectonically linked with alkalic magmatic activity (Fig. 1) (Olson et al., 1977; Larson et al., 1985; Pivarunas and Meert, 2019).

Plutonic Rocks in the Wet Mountains

The McClure Mountain Complex partly comprises older mafic and ultramafic igneous rocks which are primarily layered cumulate rocks (formed when high-temperature igneous crystals accumulated at the base of a magma chamber) (Shawe and Parker, 1967). These rocks include gabbro and pyroxenite. The younger intrusions include biotite hornblende syenite, nepheline syenite, and pyroxene nepheline syenite (also termed ijolite) (Olson et al., 1977; Magnin et al., 2023) (Fig. 4).

The Gem Park Complex is located several kilometers southwest of the McClure Mountain Complex (Fig. 4). It predominantly comprises pyroxenite and gabbro of cumulate origin, exhibiting similarities to the mafic-ultramafic rock types of the McClure Mountain Complex. The Gem Park Complex shows extensive alteration across most of its exposed outcrops and is intruded by various dikes (Parker and Sharp, 1970).

The Democrat Creek Complex is located a few kilometers southeast of the McClure Mountain Complex and consists predominantly of intrusions of quartz syenite, with a smaller gabbroic mass that is present in the southern part of the complex (Olson et al., 1977) (Fig. 4).

Powderhorn Alkalic Complex

The extensive Powderhorn Alkalic Complex (Fig. 5) contains pyroxenite as the oldest rock unit, which is intruded by a rare alkaline igneous rock termed uncompahgrite. Nepheline syenite and pyroxene-nepheline syenite (ijolite) are also present in the northeast part of the complex. Carbonatite is the youngest major intrusion within the complex (carbonatite is a rare igneous rock that consists almost entirely of carbonate minerals), and it forms a prominent hill at the center of the complex (Fig. 6). The carbonatite is intruded by younger diabase dikes, which represent sheets of slowly cooled basaltic magma (Fig. 5). (Olson et al., 1977; Olsen and Hedlund, 1981; Van Gosen, 2009).

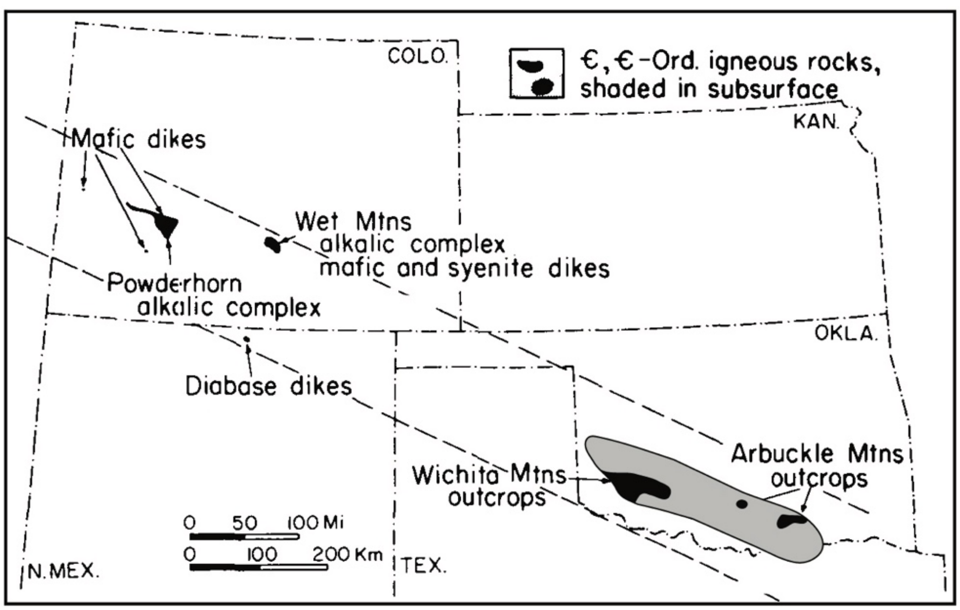

Fig. 1. Distribution of Cambrian-Ordovician igneous rocks in New Mexico, Colorado, and Oklahoma. Modified from Larson et al. (1985).

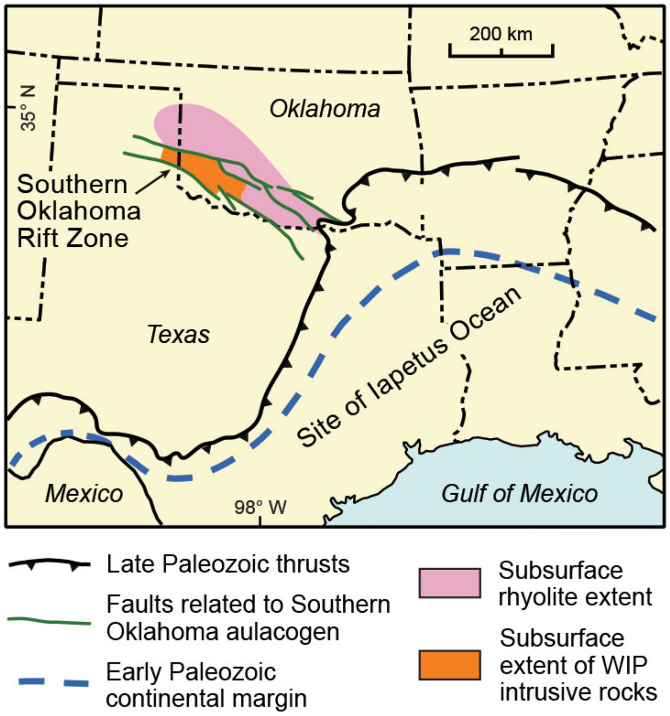

Fig. 2. Distribution of Cambrian Igneous Rocks in the Southern Oklahoma rift zone. Modified from Wall et al. (2021).

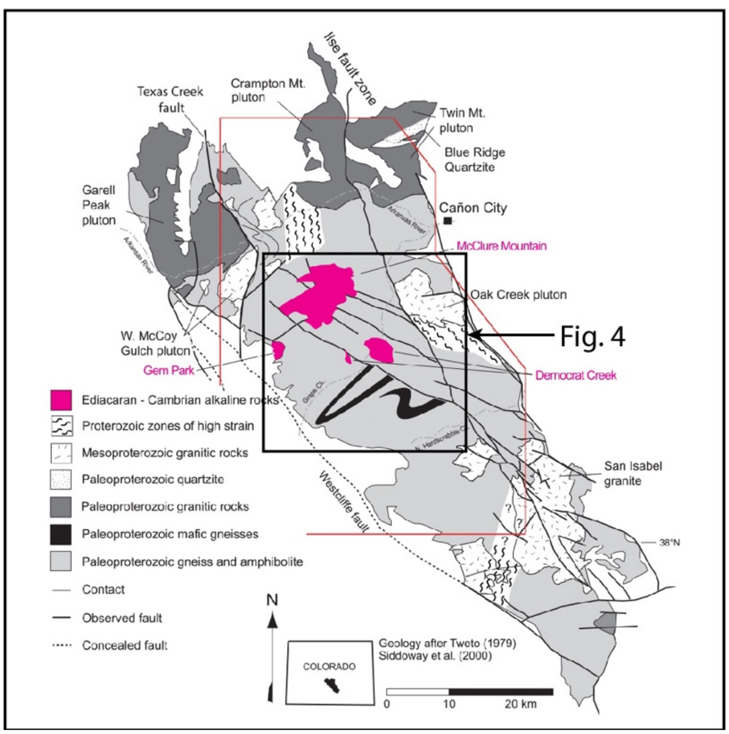

Fig. 3. General geology of the Wet Mountains with main plutonic intrusions highlighted. Modified from Magnin et al. (2023). The box indicates the location of Figure 4.

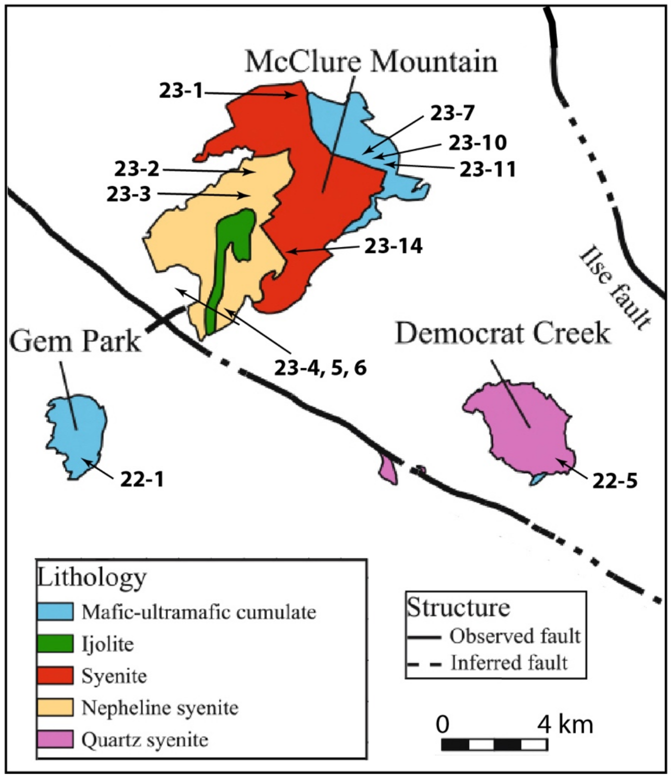

Fig. 4. Rock types of the main plutonic intrusions in the Wet Mountains. Modified from Magnin et al. (2023). Sample locations are indicated.

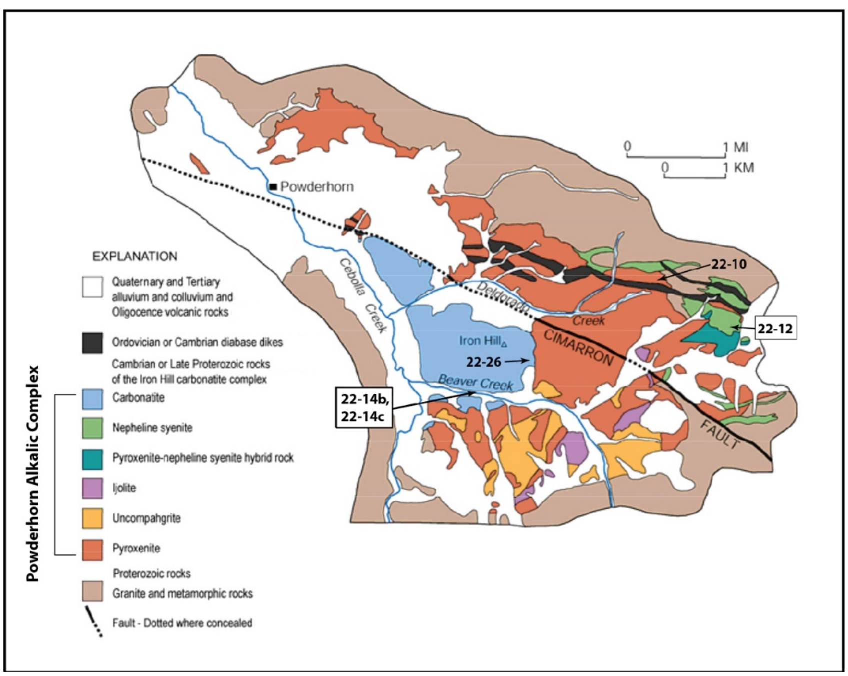

Fig. 5. Geologic map of the Powderhorn Complex. Modified from Van Gosen (2009). Sample locations are indicated.

Fig. 6. View of Powderhorn Complex showing Iron Hill Carbonatite. From Van Gosen (2009).

Methods

Samples were collected in Colorado in 2022 and 2023 by Dr. Hanson and TCU students Weston Scott and Caleb Perkey. The samples were sent out for thin-section preparation and geochemical analyses. Microscopic studies of the igneous rocks were carried out on the thin sections (Fig. 7), including the identification of igneous minerals and their alteration products, as well as a description of igneous textures. I used a petrographic microscope in this work (Fig. 8). The microscope employs two polarizing filters, the polarizer, and the analyzer. The polarizer is located beneath the stage of the microscope and allows light to vibrate in only one direction as it passes through the thin section. The analyzer is located above the objective lens and allows light vibrating 90 degrees from the polarizer to pass through it. As polarized light passes through the thin section it interacts with the minerals revealing their unique optical properties such as pleochroism and birefringence (Nesse, 2013). These optical properties assist in identifying the minerals within a thin section. All thin sections used are 0.03 mm thick and 4.5 cm in length (Fig. 7).

Samples for geochemical analysis were prepared at TCU by crushing large rock samples and separating out weathered or altered material. To obtain a statistically representative portion of each sample weighing 200g, the cone and quartering technique was used. The resulting 200g was sent to Washington State University for geochemical analysis. Major elements and some trace elements were analyzed by X-ray fluorescence spectrometry and a complete suite of trace elements was analyzed by inductively coupled plasma-emission mass spectrometry.

Fig. 7. Example of a thin section (4.5 cm long).

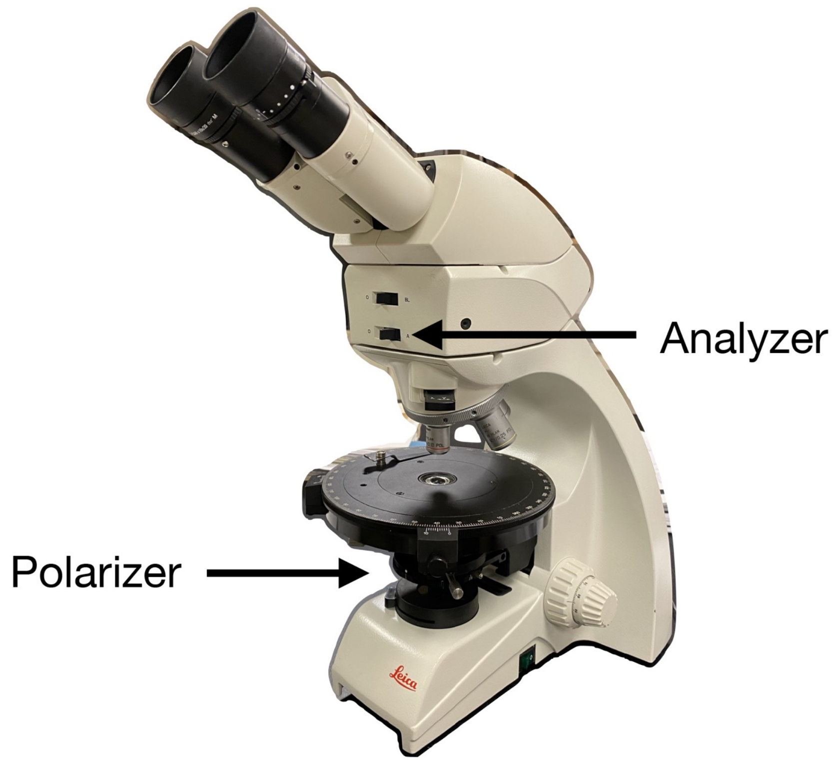

Fig. 8. Standard petrographic microscope using polarized light.

Microscopic Studies

McClure Mountain Complex

We have three samples from the layered mafic-ultramafic intrusive rocks within the McClure Mountain Complex. Samples CO23-10 (Figs. 9 and 10) and CO23-11 are gabbros from the layered intrusion and show little alteration. The dominant minerals consist of olivine, augite, and plagioclase. Augite partially replaces olivine, indicating that olivine formed first and then started reacting with the cooling magma. These are cumulate rocks that were formed by the accumulation of minerals on the floor of the magma chamber. Sample CO23-7 comes from massive pyroxenite (Fig. 11) that intruded the cumulate rocks and consists almost entirely of coarse-grained augite. Small amounts of kaersutite partially replace the augite (Figs. 12 and 13).

Sample CO23-14 is a representative sample of the hornblende biotite syenite that forms a large part of the McClure Mountain Complex. This sample has abundant orthoclase showing typical exsolution lamellae of albite. Plagioclase, biotite, and apatite are less abundant, and noticeable amounts of titanite also occur. Clots of plagioclase and orthoclase are visible in the thin section and suggest an accumulation of crystals on the floor of the magma chamber (Figs. 14 and 15).

Sample CO23-1 is a sodalite nepheline syenite. The minerals consist of abundant orthoclase showing typical exsolution lamellae of albite, as well as sodalite, nepheline, and hornblende. There are minor amounts of plagioclase, cancrinite that has partly replaced nepheline, and biotite, which formed reaction rims around the hornblende. This sample comes from an area mapped as syenite (Fig. 4), but the mineralogy of the sample shows that sodalite nepheline syenite also occurs here. Samples CO23-2 (Figs. 16 and 17), CO23-3, CO23-4, and CO23-5 are typical nepheline syenites. All four samples contain subequal amounts of nepheline and orthoclase. The main mafic mineral in sample CO23-3 is aegirine. The other three samples contain hornblende with minor amounts of biotite, titanite, and apatite.

Gem Park Complex

We have one representative sample from the Gem Park Complex, CO22-1, which is a pyroxenite consisting dominantly of diopside and kaersutite (Fig. 18). Brown kaersutite is seen replacing diopside, which resulted from a reaction between higher temperature diopside and cooling magma. The kaersutite has been altered to green actinolite, which is a lower temperature mineral that formed during further cooling of the intrusion. Under reflected light, an unusual amount (~20%) of pyrite and magnetite can be seen.

Democrat Creek Complex

We also have one representative sample from the Democrat Creek Complex, CO22-5, which is a quartz syenite (Fig. 19). The dominant minerals consist of orthoclase, quartz, plagioclase, and brown hornblende. Biotite is less abundant. The orthoclase shows exsolution lamellae of albite, which is typical of igneous orthoclase and forms during cooling from magmatic temperatures. This sample shows very low degrees of alteration.

Powderhorn Alkalic Complex

We have two samples of nepheline syenite from the Powderhorn Complex. Sample CO22-10 is a nepheline syenite dike intruding the pyroxenite in the complex. It has abundant tabular orthoclase showing perthitic texture and characteristic Carlsbad twinning. Nepheline is less abundant than orthoclase, and there are minor amounts of biotite, aegirine, titanite, and apatite. Fine-grained calcite occurs as an alteration product in places. Sample CO22-12 comes from a larger intrusion of nepheline syenite farther to the east. It has very similar mineralogy and texture to CO22-10. However, sample CO22-12 shows significant alteration, with fine-grained intergrowths of muscovite, cancrinite, and natrolite partially replacing nepheline (Figs. 20 and 21).

We also have three samples of carbonatite from the Powderhorn Complex. Samples CO22-14b (Fig. 22) and CO22-14c were collected very close together along a single roadcut because they showed different appearances in hand sample. Sample CO22-26 comes from a different part of the carbonatite (Fig. 5). All three samples consist dominantly of igneous calcite and dolomite, but those minerals are difficult to tell apart microscopically. Sample CO22-14c also contains a significant amount of fine- to medium-grained apatite. Fine-grained crystals of apatite also occur in CO22-26.

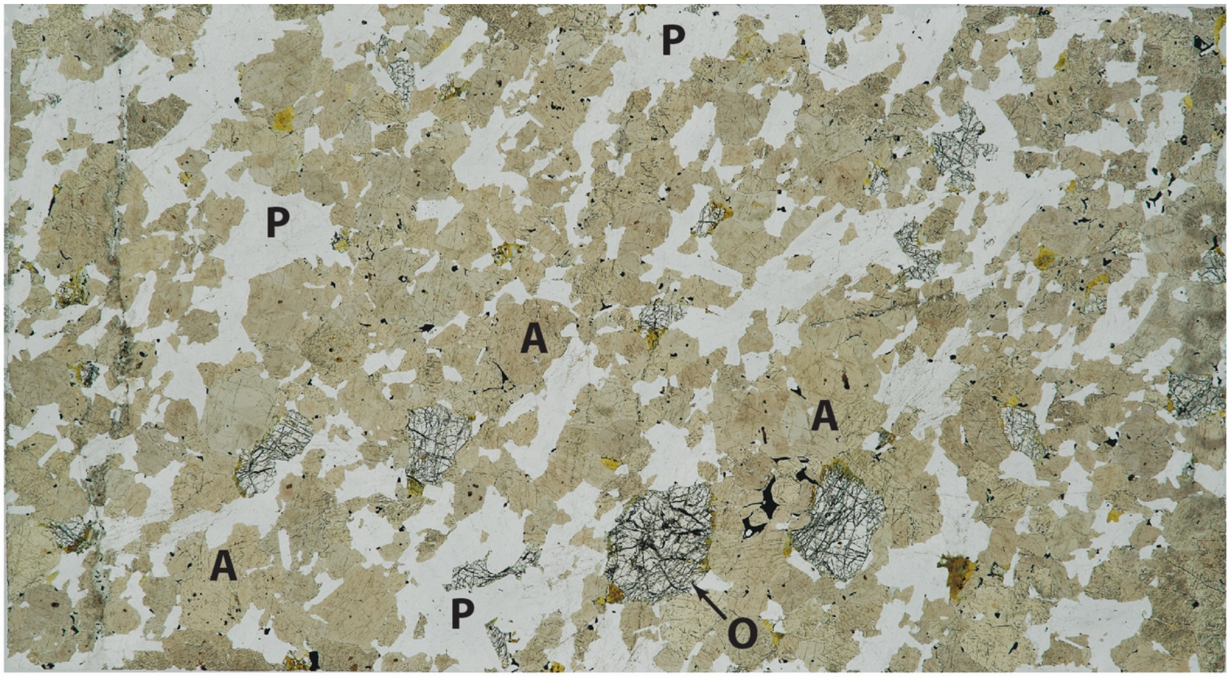

Fig. 9. **CO23-10** Photomicrograph of cumulate olivine gabbro from layered mafic intrusion in McClure Mountain Complex. A=augite, O=olivine, and P=plagioclase. Plane light. Width of view 4cm.

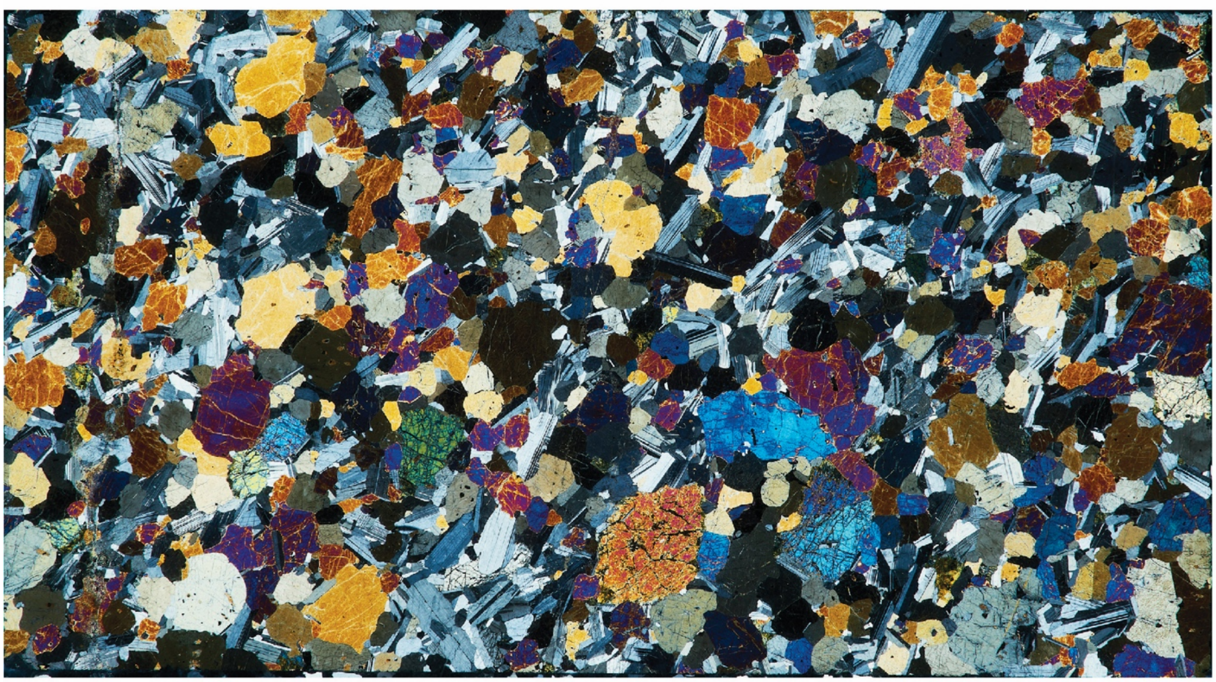

Fig. 10. **CO23-10** Same view in crossed polars.

Fig. 11. Cumulate pyroxenite from layered mafic intrusion in McClure Mountain Complex. Pencil for scale.

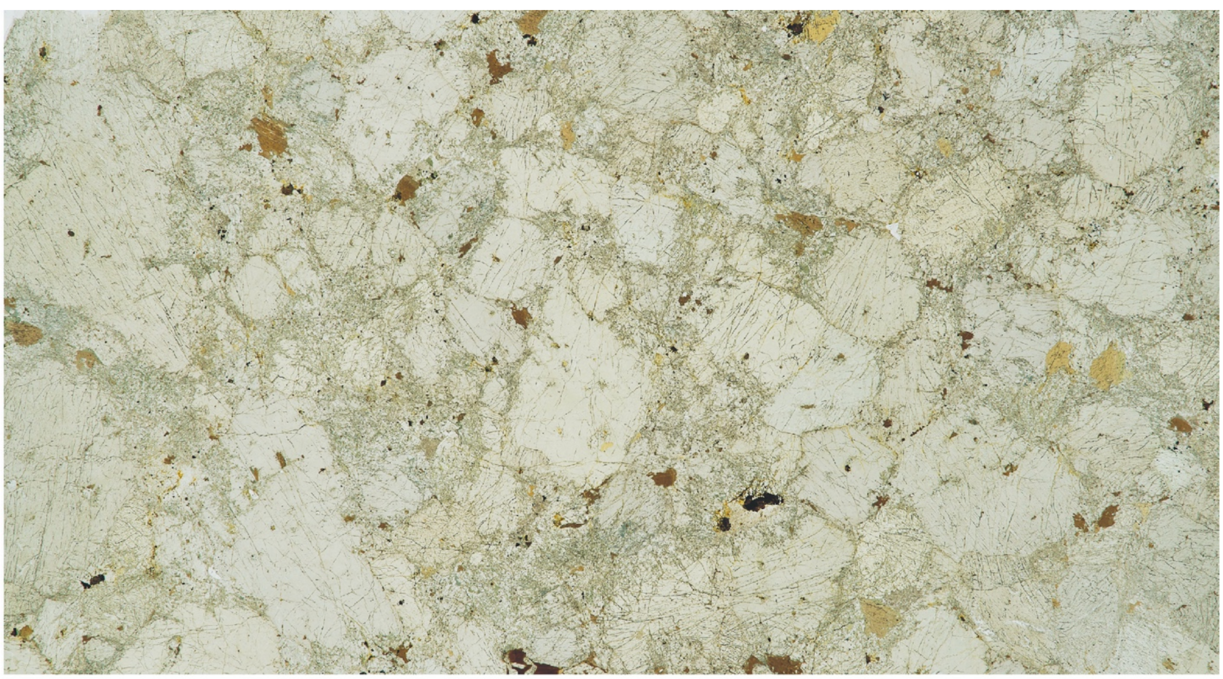

Fig. 12. **CO23-7** Photomicrograph of pyroxenite from the McClure Mountain Complex. The clear areas are Diopside and the brown and yellow minerals are kaersutite. Plane light. Width of view 4cm.

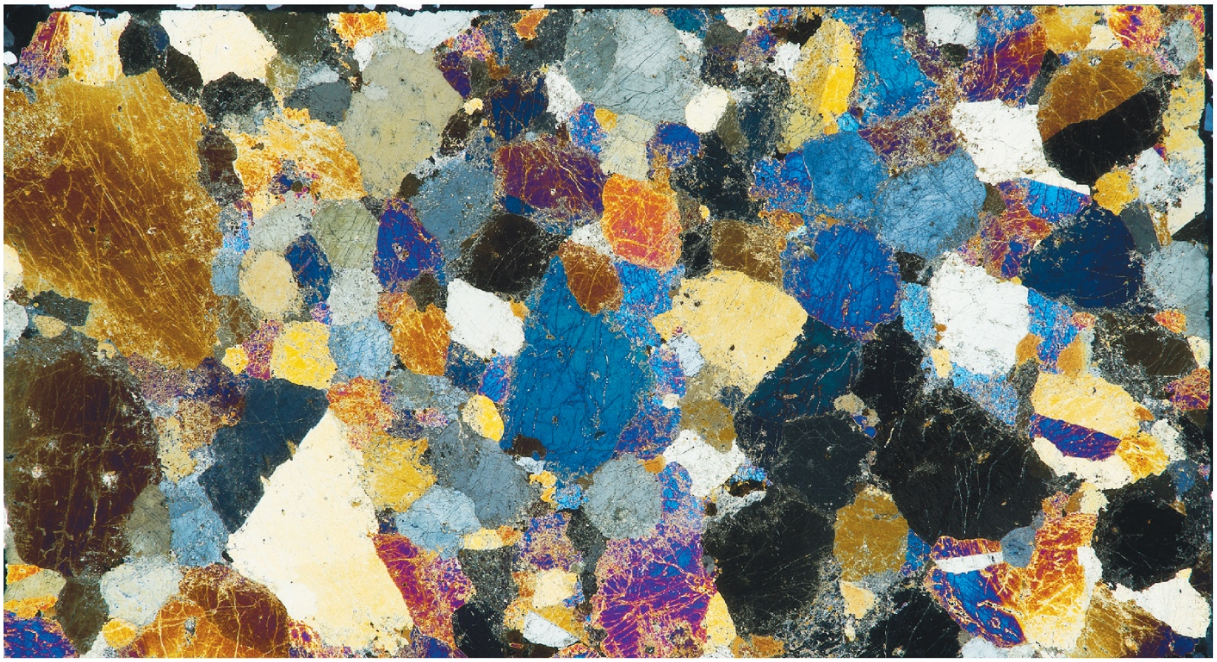

Fig. 13. **CO23-7** Same view in crossed polars.

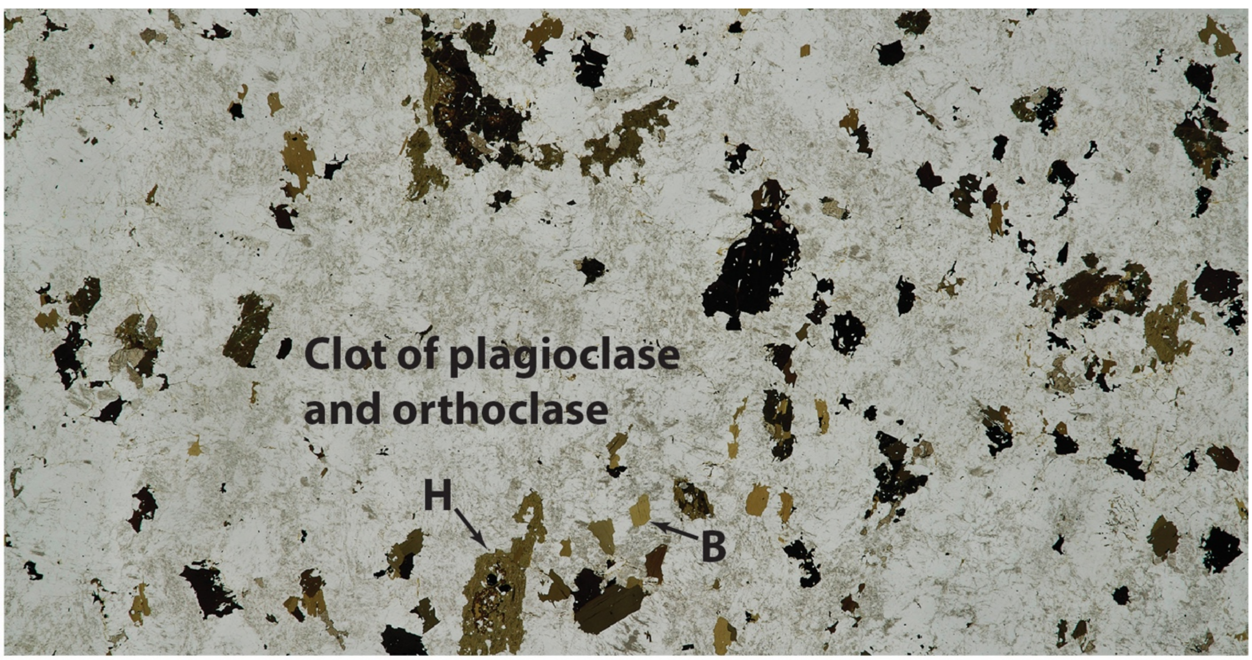

Fig. 14**. CO23-14** Photomicrograph of syenite from the McClure Mountain Complex. H=Hornblende, B=Biotite, and the colorless minerals are orthoclase and plagioclase. Plane light. Width of view 4cm.

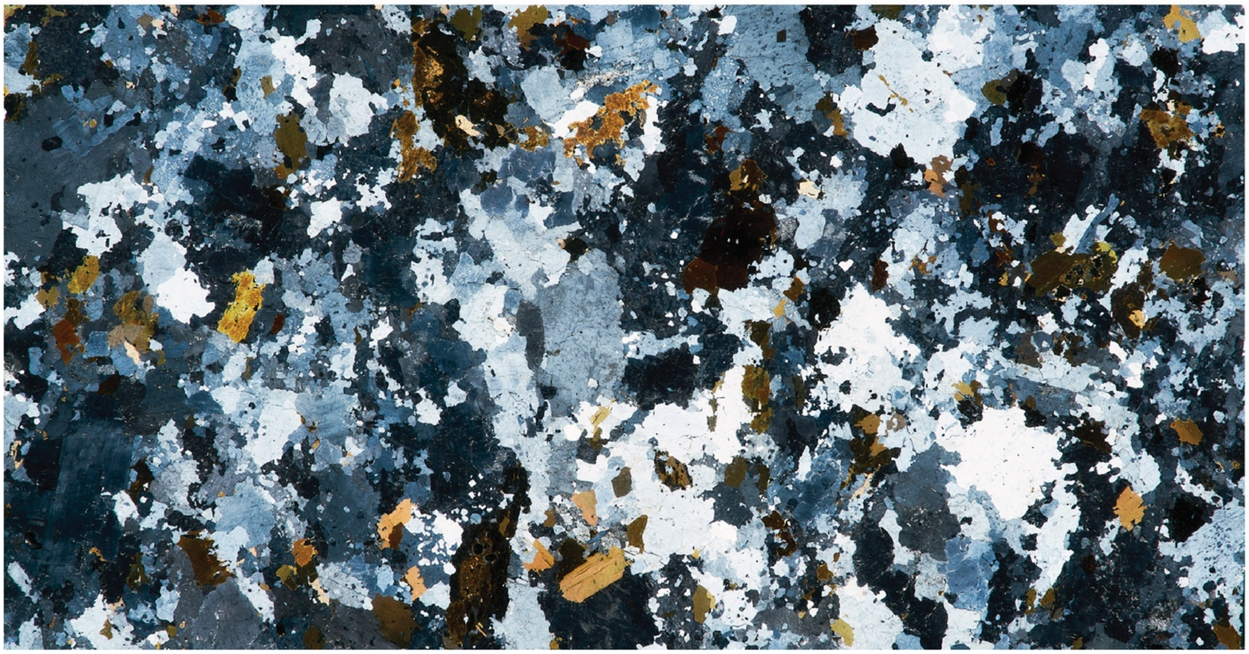

Fig. 15. **CO23-14** Same view in crossed polars.

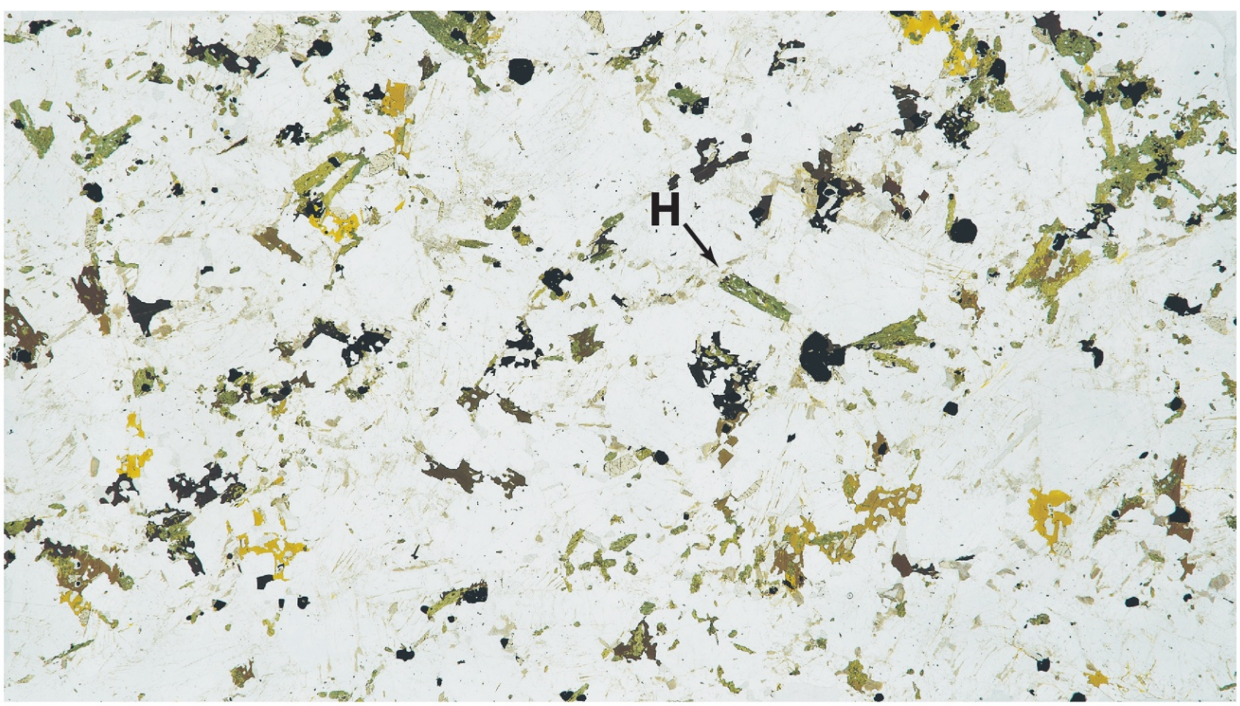

Fig. 16. **CO23-2** Photomicrograph of nepheline syenite in the McClure Mountain Complex. H=Hornblende. Plane light. Width of view 4cm.

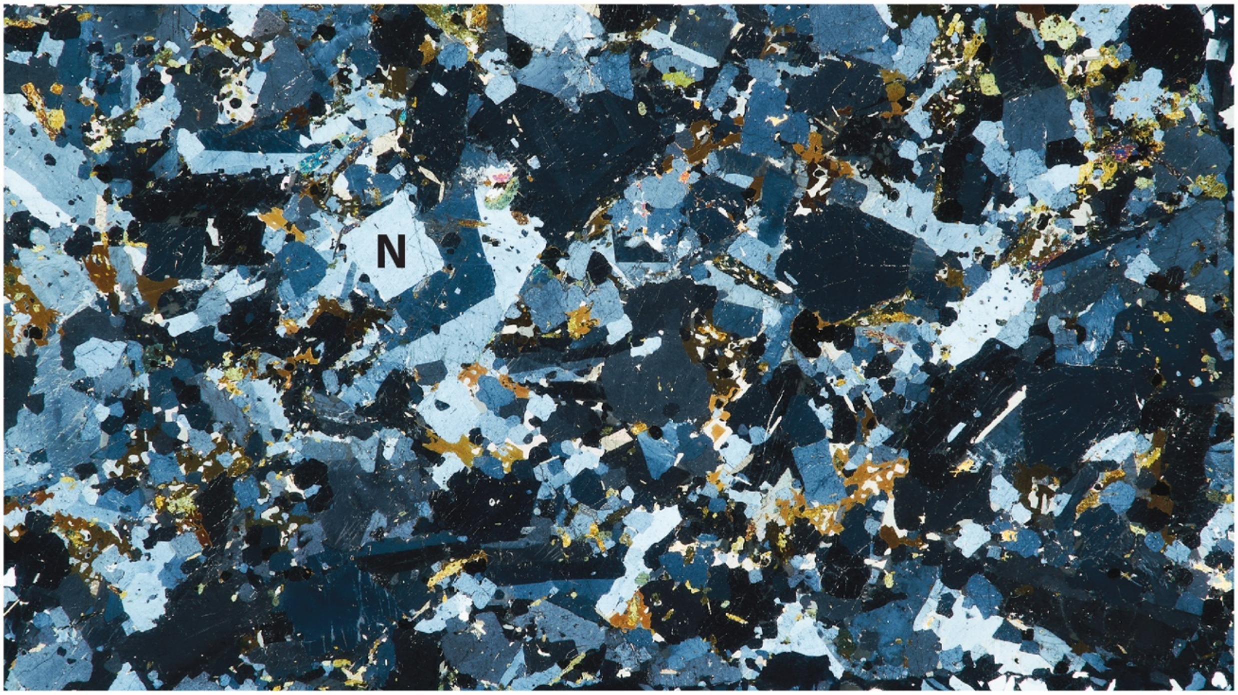

Fig. 17**. CO23-2** Same view in crossed polars. N=nepheline.

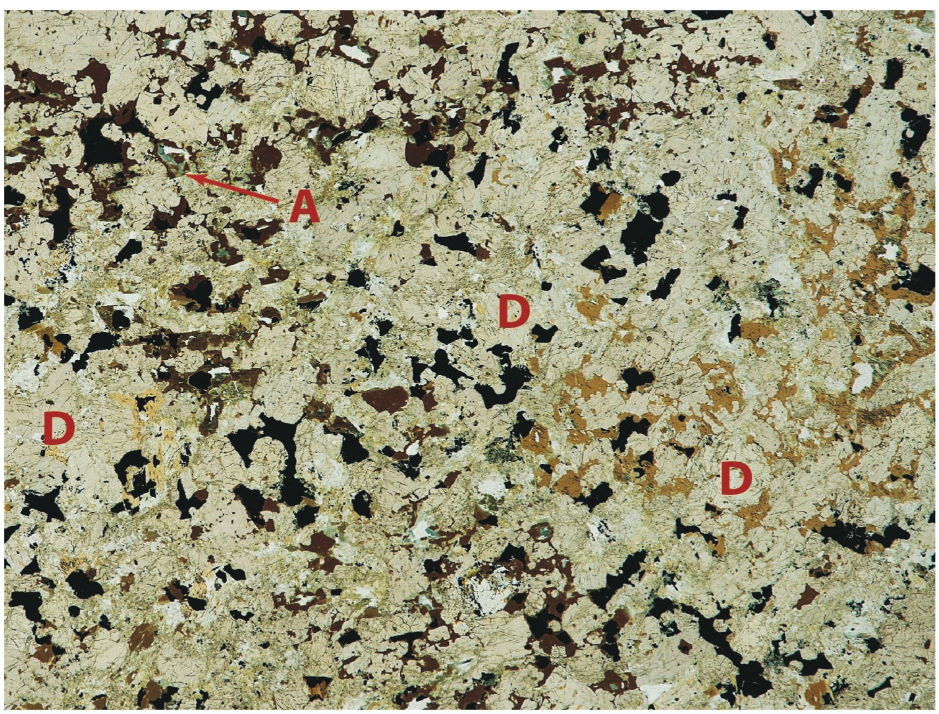

Fig. 18. **CO22-1** Photomicrograph of cumulate pyroxenite from the Gem Park Complex showing brown kaersutite replacing diopside (D). A=actinolite. Plane light. Width of view 2.5cm.

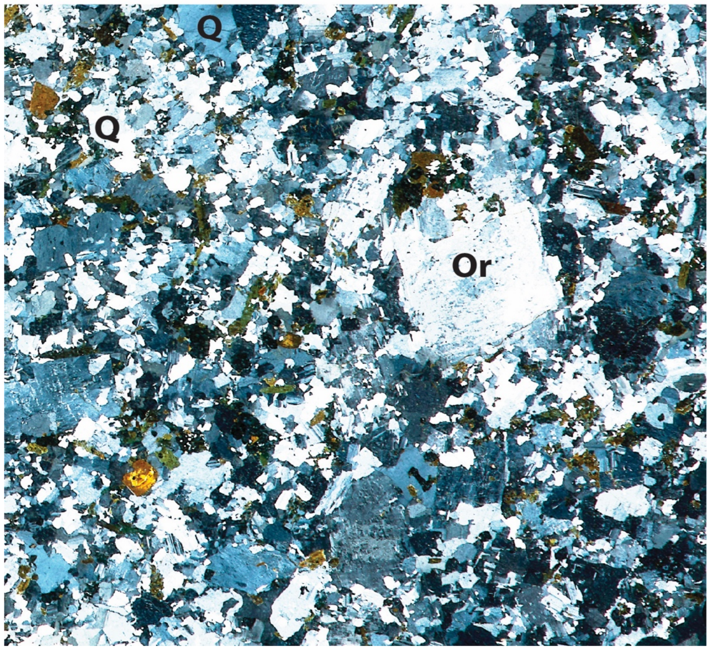

Fig. 19. **CO22-5** Photomicrograph of quartz syenite from Democrat Creek Complex. Or=orthoclase, Q=quartz. Crossed polars. Width of view 1.3cm.

Fig. 20. **CO22-12** Photomicrograph of nepheline syenite from the Powderhorn Complex. Lightly colored areas are nepheline and orthoclase. Plane Light. Width of view 4cm.

Fig. 21. **CO22-12** Same view in crossed polars. Bright areas are alteration products of nepheline.

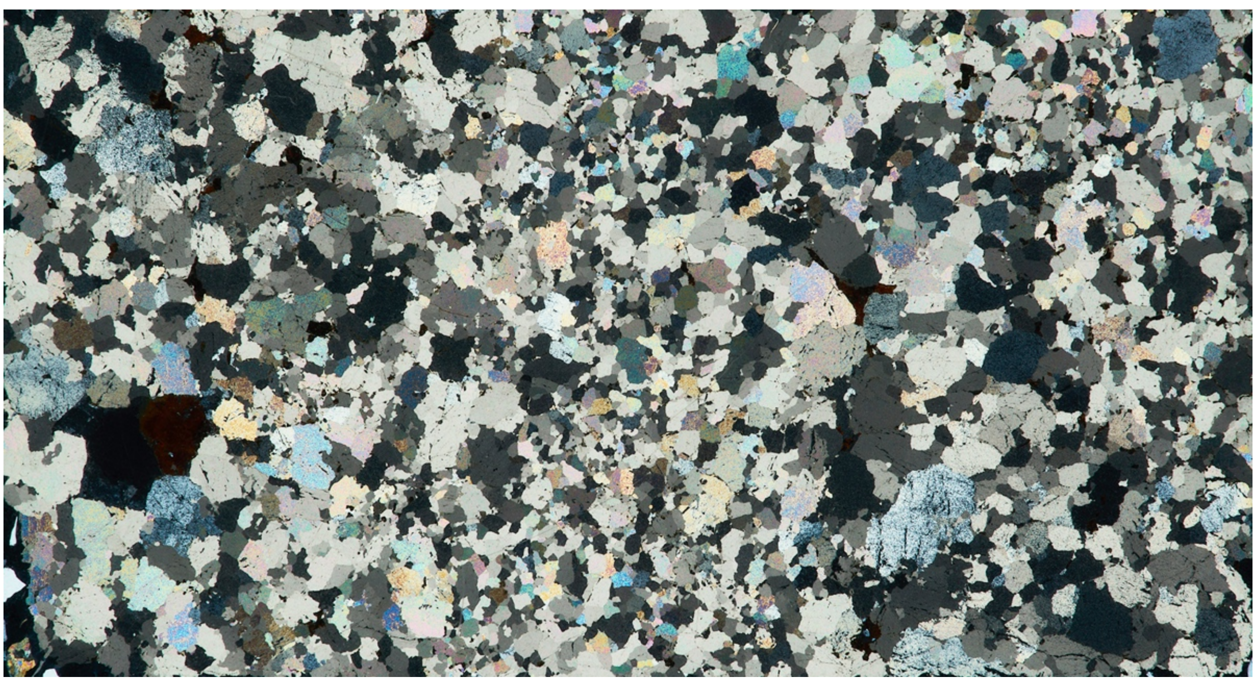

Fig. 22. **CO22-14b** Photomicrograph of carbonatite from the Powderhorn Complex. Different colors represent carbonate minerals cut in different orientations by the thin section. Crossed polars.Width of view 4cm.

Geochemistry

Here I follow standard procedures in igneous geochemistry, in which the major elements are reported as oxides in weight percent. Trace elements are reported in parts per million (ppm). The data are shown on Harker diagrams, which plot concentrations of major oxides and trace elements compared to silica (SiO_2), because silica generally increases during the evolution of related magmas. These diagrams are widely used in studies of igneous rocks to show possible genetic relationships (Rollinson and Pease, 2021). Trace elements are also plotted on normalized multi-element diagrams. In these diagrams, trace element values in the samples are divided by average values for the primitive mantle, which represents the composition of the original Earth's mantle after the initial formation of the planet (Sun and McDonough, 1989). This provides a convenient way to compare trace element contents of igneous rock samples from different settings. Rare earth elements (REE) can also be used in this way by normalizing their values to average chondrites (a primitive type of meteorite). These elements are very sensitive to igneous processes and they are plotted in order of atomic number and atomic weight (Sun and McDonough, 1989). Samples that are closely related should show similar REE patterns.

McClure Mountain Complex

Data from the McClure Mountain Complex are plotted on Harker diagrams in Figures 23-30. Two cumulate gabbro samples from the McClure Mountains layered complex (CO23-10 and CO23-11) have almost identical CaO, FeO, TiO_2, MgO, Ni, and Cr contents, even though they were collected from different locations (Figs. 23-26, 29 and 30). Their REE patterns are also nearly identical (Fig. 31), as are their patterns on the multi-element diagram (Fig. 32). The close geochemical similarities between these two samples indicate that the magma composition in the chamber remained constant at certain times during the formation of the crystals.

The third sample from the layered complex is CO23-7, which is a pyroxenite and is compositionally different in most of the major oxides and trace elements relative to samples CO23-10 and CO23-11, as seen in the Harker diagrams (Figs. 23-30). This sample also shows higher Ni and Cr contents and somewhat different patterns on the REE and multi-element diagrams (Figs. 31 and 32). The field relationships show that this rock type formed from magma that intruded the gabbros. It represents mafic magma that formed at a deeper level and was then injected into the cumulate rocks (Shawe and Parker, 1967). The differences in trace element content indicate that it comes from a different batch of magma.

Sample CO23-14 is a syenite that forms a large part of the McClure Mountain Complex. This sample is relatively low in K_2O (Fig. 27) and high in TiO_2 (Fig. 23) compared to the nepheline syenites. It also has a very different REE pattern with generally low REE contents but with a strong positive Eu anomaly (Fig. 33) and a strong positive Ba anomaly (Fig. 34). Eu is compatible with both plagioclase and orthoclase and barium is highly compatible with orthoclase. Therefore, it appears that this sample is a cumulate rock where orthoclase and plagioclase were accumulating on the floor of the magma chamber. These results are consistent with microscopic observations of the sample.

Sample CO23-1 is a sodalite-nepheline syenite and samples CO23-2, CO23-3, CO23-4, and CO23-5 are nepheline syenites. These samples show a wide range of silica content on the Harker diagrams (Figs. 23-30). There is no obvious trend shown by all the samples that would indicate that they all represent evolving magmas from an original starting magma. However, samples CO23-3 and CO23-4 have very similar REE patterns indicating that these two samples could be genetically related (Fig 33). In contrast, samples CO23-1, CO23-2, and CO23-5 have different REE patterns indicating that they are not directly related to each other (Fig. 33). Sample CO23-1 shows a very strong negative Eu anomaly indicating fractionation of plagioclase occurred. A strong negative Ba anomaly can also be seen that is consistent with the fractionation of K-feldspar and plagioclase from a precursor magma (Fig. 34). Sample CO23-4 also shows a weaker negative Eu anomaly that is still consistent with some fractionation of plagioclase (Fig. 33). In contrast, sample CO23-5 shows a very different REE pattern. It is lower in total REE than the rest of the samples. This sample shows a strong positive Eu anomaly (Fig. 34) indicating that it is a cumulate rock that formed when crystals were settling to the floor of the magma chamber.

Samples CO23-2, CO23-3, CO23-4, and CO23-5 all come from a limited area in the McClure Mountain Complex. The first three samples CO23-2, CO23-3, and CO23-4 overall could be genetically related due to their similarities in the REE patterns, but CO23-5 has a very different REE pattern indicating that it represents a separate pulse of magma that was injected from deeper levels. The syenite sample CO23-14 has a distinctly different geochemistry because it is silica-saturated and shows a strong positive Eu anomaly which suggests it represents a cumulate rock that must also be originating from a different part of the magma chamber.

Gem Park Complex

Sample CO22-1 has the highest TiO_2, FeO, and Ni content of any of the samples collected from the Wet Mountains (Figs. 23, 25, and 29). These elements are likely contained in the opaque phases pyrite and magnetite, which are unusually abundant in this sample. MgO and CaO contents are also high (Figs. 24 and 26), which is consistent with the cumulate origin of the Gem Park Complex.

Democrat Creek Complex

Sample CO22-5 has the highest SiO_2 content on the Harker diagrams with low TiO_2, MgO, and CaO contents compared to most of the other samples (Figs. 23, 24, and 26), indicating that it represents a highly evolved magma. The high SiO_2 content is consistent with the fact that this is the only sample that shows quartz in thin section. The sample shows highly fractionated patterns on the REE element and the multi-element diagrams (Figs. 35 and 36).

Powderhorn Complex

In Figures 37-45, I plot the major oxides TiO_2, MgO, FeO, CaO, K_2O, Na_2O, P_2O_5, and the trace elements Ni and Cr on Harker variation diagrams for the five samples collected in the Powderhorn Complex. Note that the X-axis on the diagrams has been expanded. A large gap between the carbonatites and the silicate igneous rocks in these diagrams indicates that there is no direct genetic relationship between the two igneous groups, which is commonly the case (Jones et al., 2013). The main constituents of the carbonatite samples are FeO, MgO, and CaO. The Ca and Mg are contained in calcite and dolomite, two of the most common minerals in carbonatites, and the Fe is likely substituting for Mg in the dolomite. Samples CO22-14b and CO22-14c were collected very close together along the same roadcut and have very similar geochemical compositions, except for P_2O_5 (Fig. 43). In contrast, sample CO22-26 is significantly different on almost all of the Harker diagrams, suggesting that it represents a separate patch of magma. Although samples CO22-14b and CO22-14c are generally geochemically similar, CO22-14b is much higher in P_2O_5. Phosphorus usually occurs in carbonatites in the form of the mineral apatite, which is abundant in sample CO22-14b. This indicates that even on the scale of a single outcrop different pulses of magma were intruded within the same small area with different amounts of apatite present in different pulses.

Sample CO22-26 was collected from a different part of the carbonatite and shows very different major oxides, especially MgO. The trace elements Cr and Ni also have different contents (Figs. 37-45). All three samples have light REE-enriched patterns typical of carbonatites in general but sample CO22-14b has lower total REEs than the other two samples (Fig. 46). This is most likely due to the low content of apatite in that sample because apatite is one of the main minerals that contains P_2O_5.

The two nepheline syenites samples from the Powderhorn complex plot very close together on almost all the Harker variation diagrams except for K_2O (Fig. 41), indicating they represent closely related magmas. K_2O is noticeably higher in sample CO22-12 compared to CO22-10, which reflects the higher degree of alteration of the former sample, including the presence of abundant secondary muscovite. The two samples have very similar heavy REE patterns and show positive Eu anomalies indicating some accumulation of feldspar. In sample CO22-12 the light REEs are unusually low and that most likely indicates a disturbance of those elements by alteration (Fig. 47). The patterns for the two samples on the multi-element diagram are similar except for the lower right part which again could be a result of the alteration of sample CO22-12 (Fig. 48).

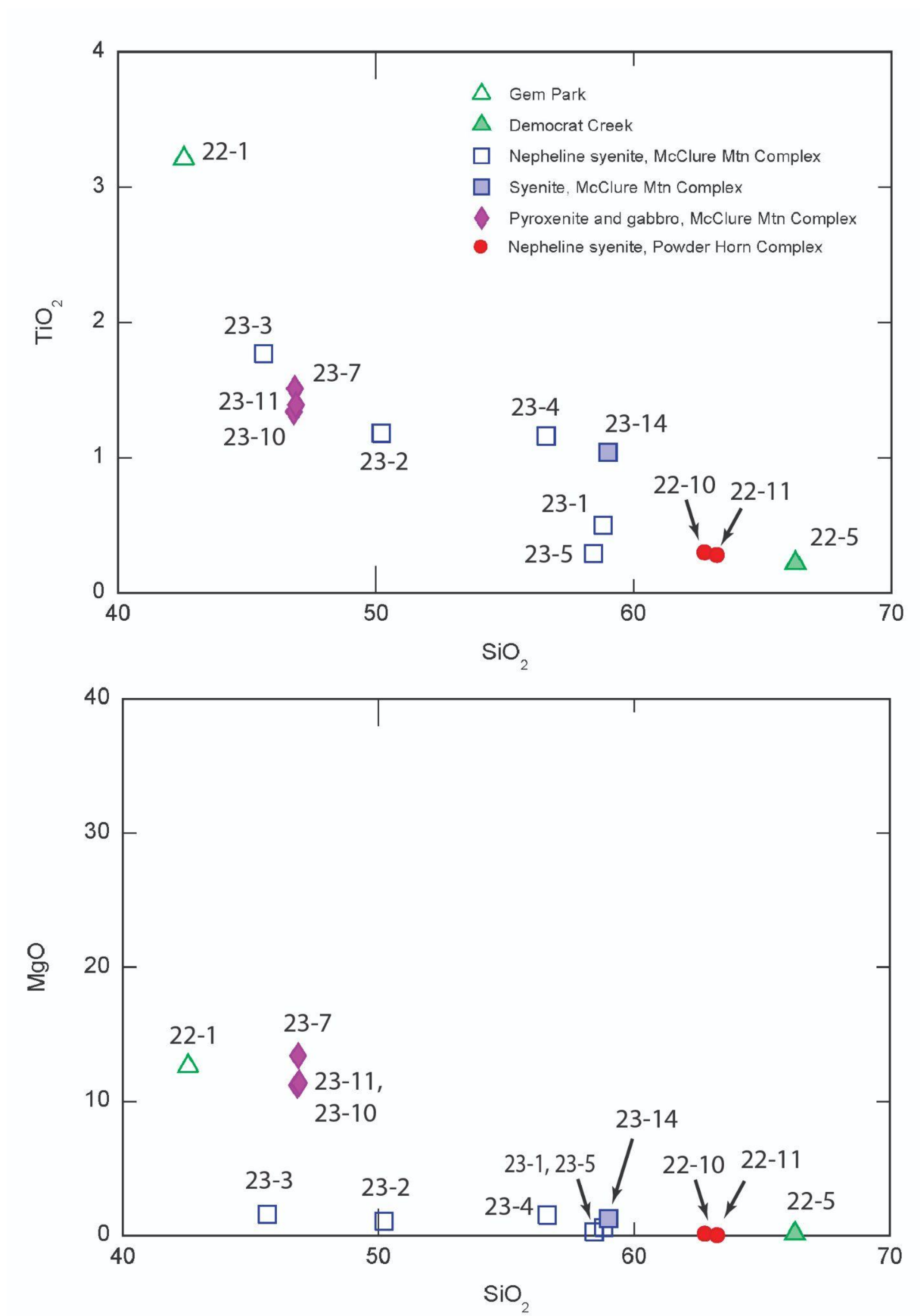

Fig. 23. (Upper Figure) TiO_2 Harker variation diagram with oxides in weight percent.

Fig. 24. (Lower Figure) MgO Harker variation diagram with oxides in weight percent.

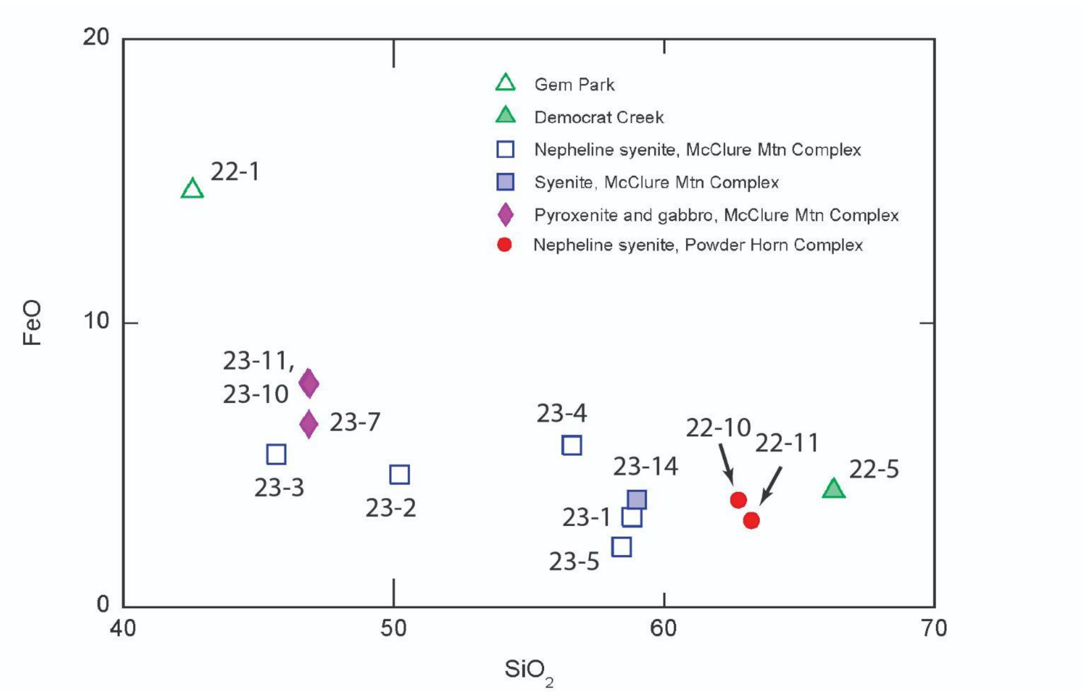

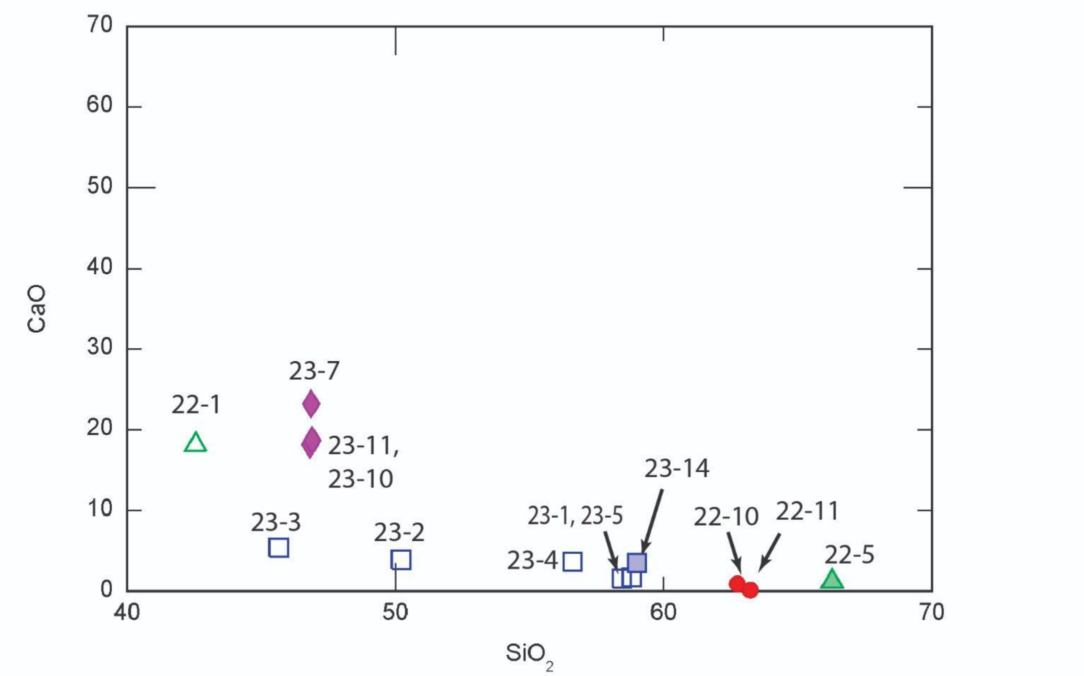

Fig. 25. (Upper Figure) FeO Harker variation diagram with oxides in weight percent.

Fig. 26. (Lower Figure) CaO Harker variation diagram with oxides in weight percent.

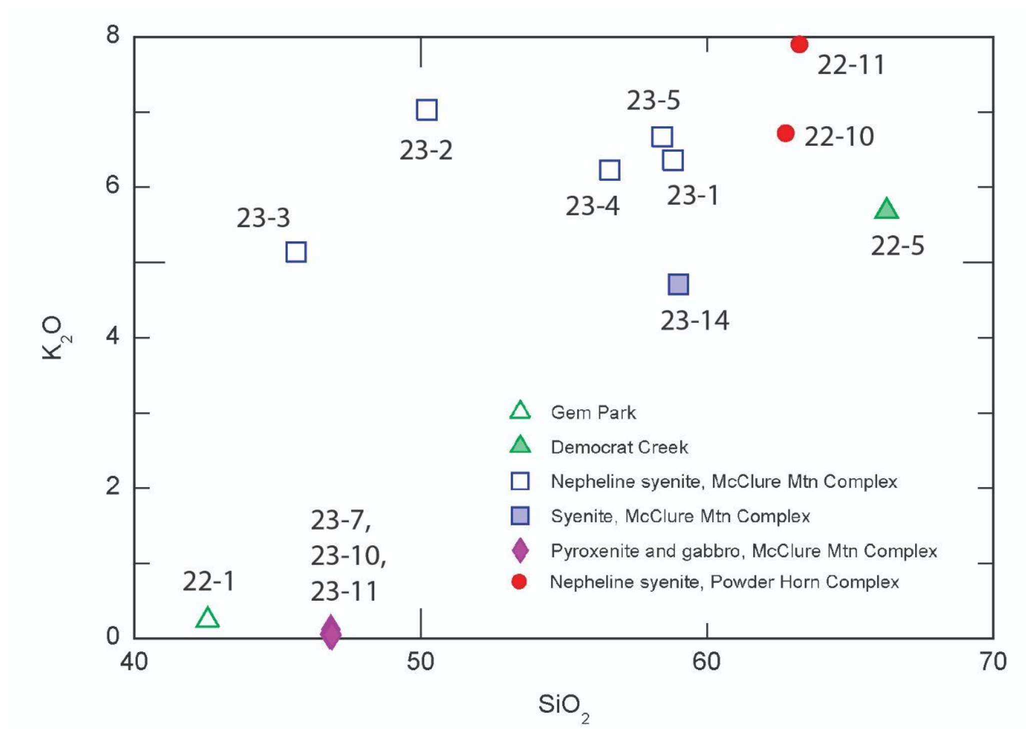

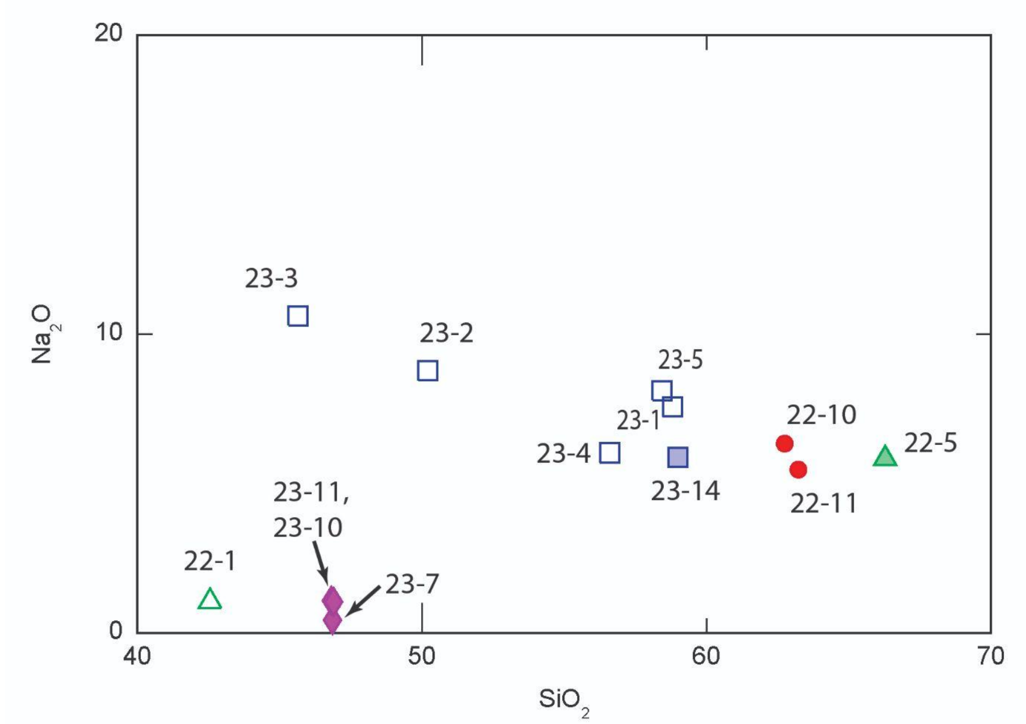

Fig. 27. (Upper Figure) K_2O Harker variation diagram with oxides in weight percent.

Fig. 28. (Lower Figure) Na_2O Harker variation diagram with oxides in weight percent.

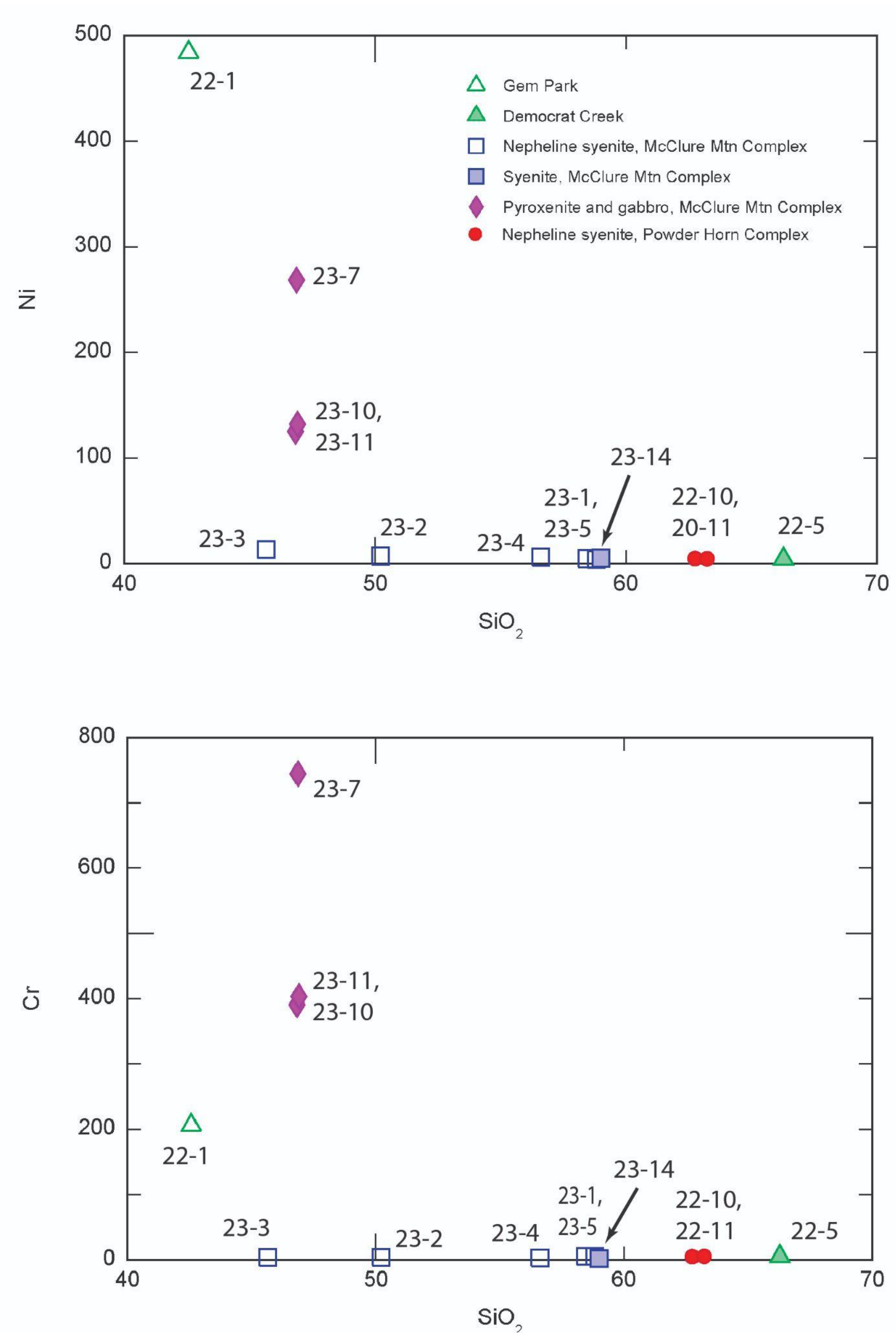

Fig. 29. (Upper Figure) Ni Harker variation diagram with silica in weight percent and Ni in ppm.

Fig. 30. (Lower Figure) Cr Harker variation diagram with silica in weight percent and Cr in ppm.

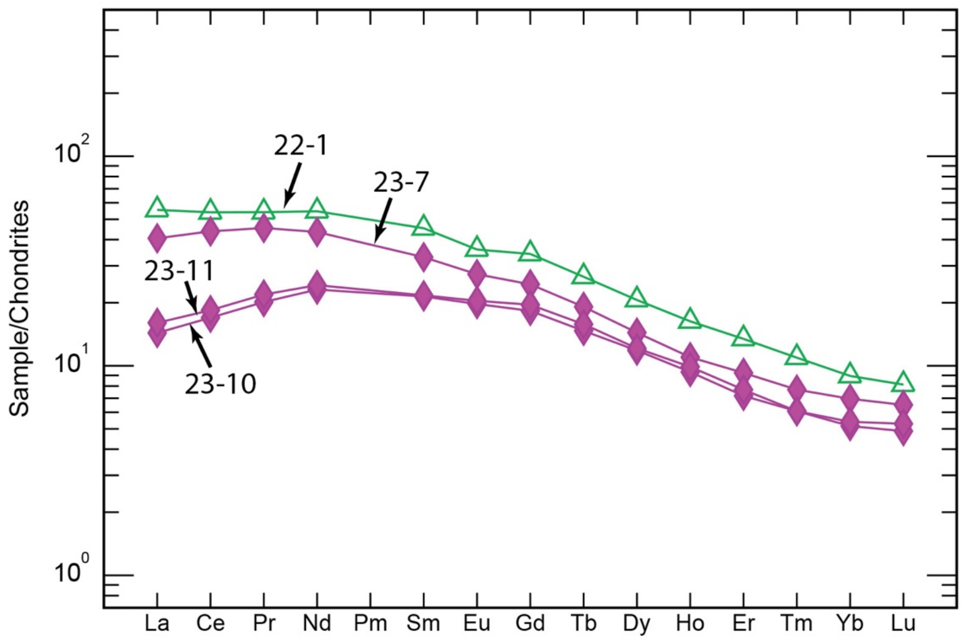

Fig. 31. REE element patterns for olivine gabbro and pyroxenite in the McClure Mountain Complex and for pyroxenite in the Gem Park Complex. Refer to Figure 29 for an explanation of symbols.

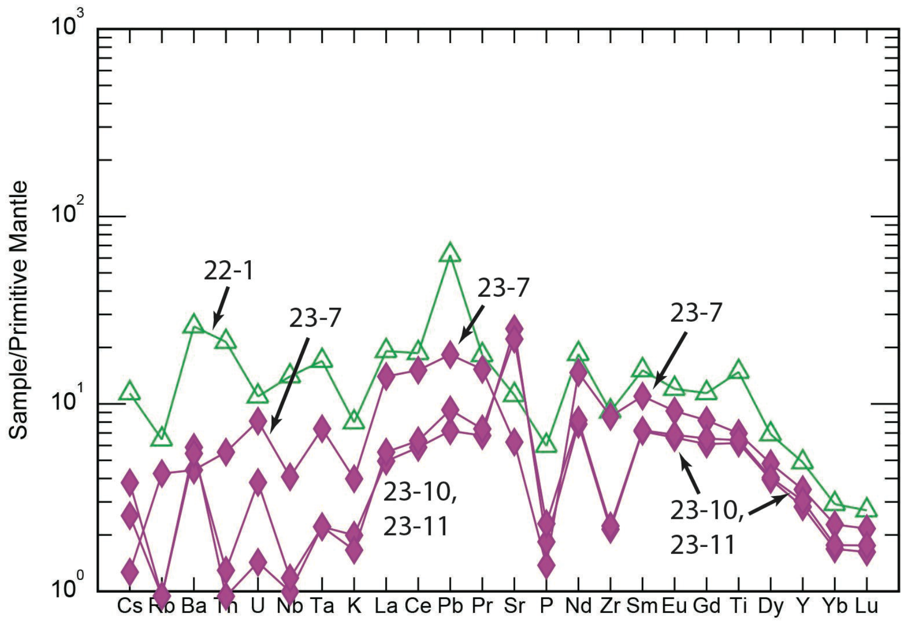

Fig. 32. Multi-element diagram for olivine gabbro and pyroxenite in the McClure Mountain Complex and for pyroxenite in the Gem Park Complex. Refer to Figure 29 for an explanation of symbols.

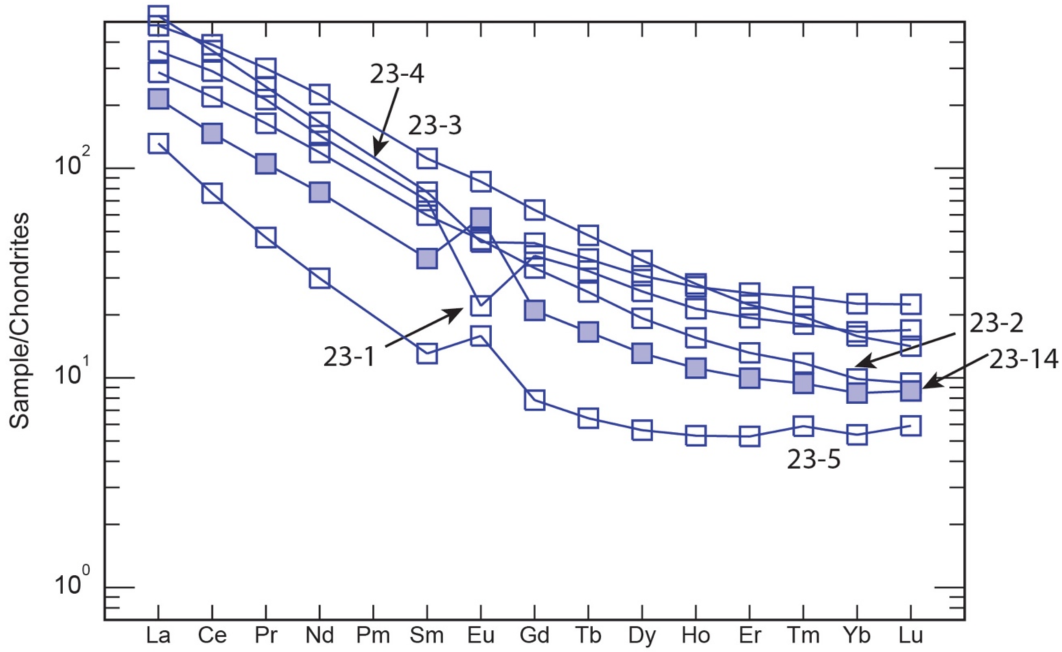

Fig. 33. REE element patterns for sodalite nepheline syenite, nepheline syenite, and syenite in the McClure Mountain Complex. Refer to Figure 29 for an explanation of symbols.

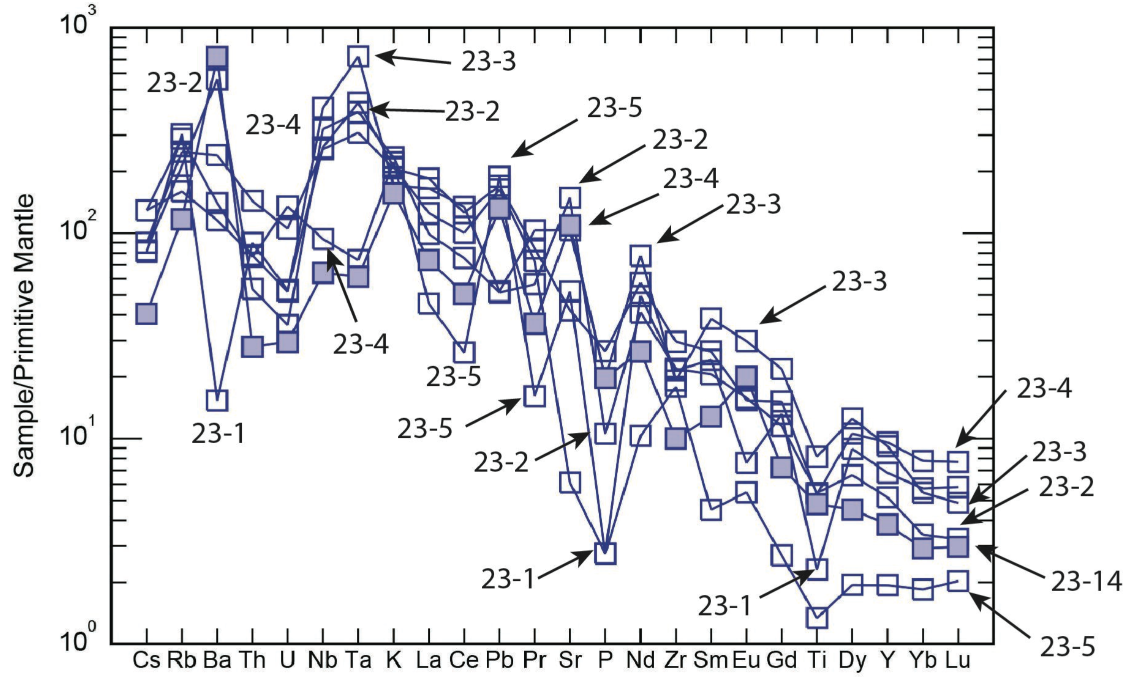

Fig. 34. Multi-element diagram for sodalite nepheline syenite, nepheline syenite, and syenite in the McClure Mountain Complex.

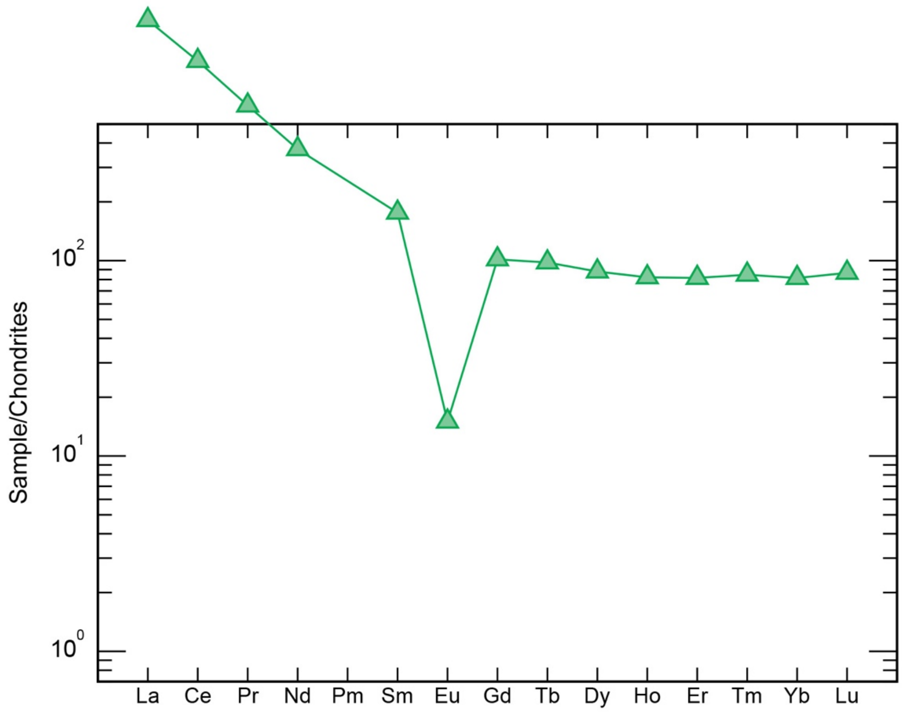

Fig. 35. REE element pattern for the Democrat Creek Complex.

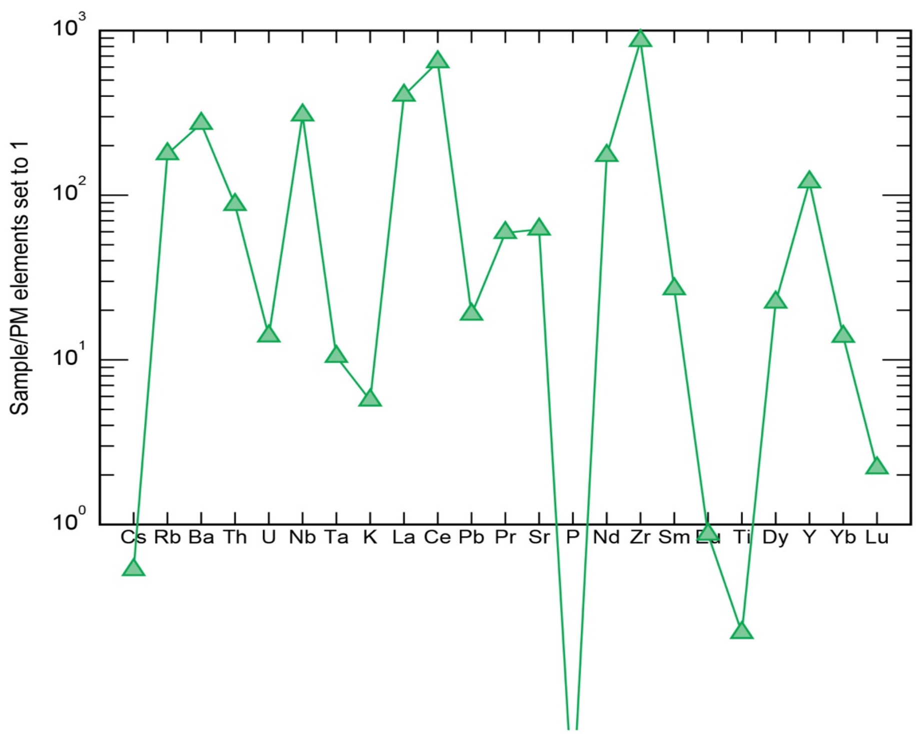

Fig. 36. Multi-element diagram for the Democrat Creek Complex.

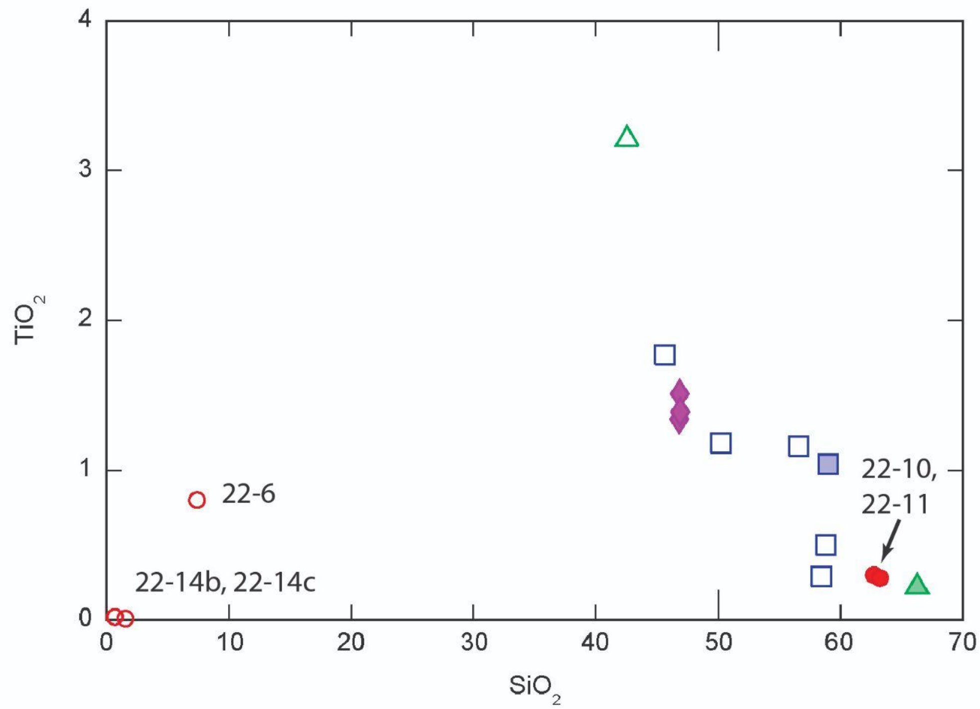

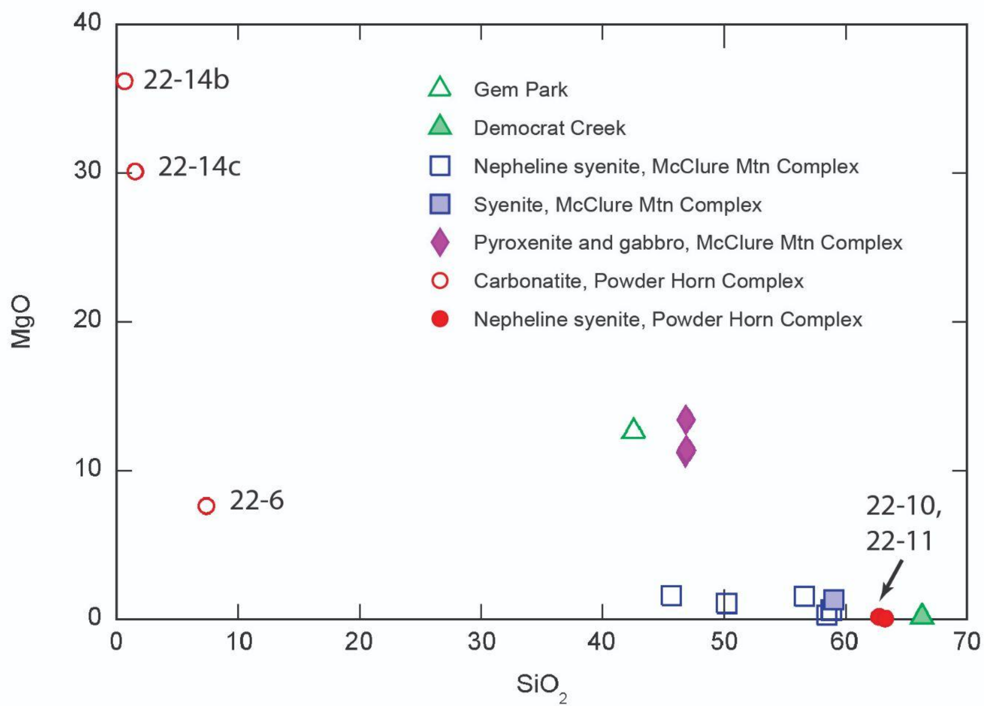

Fig. 37. (Upper Figure) TiO_2 Harker variation diagram with oxides in weight percent. Powderhorn samples labeled.

Fig. 38. (Lower Figure) MgO Harker variation diagram with oxides in weight percent.

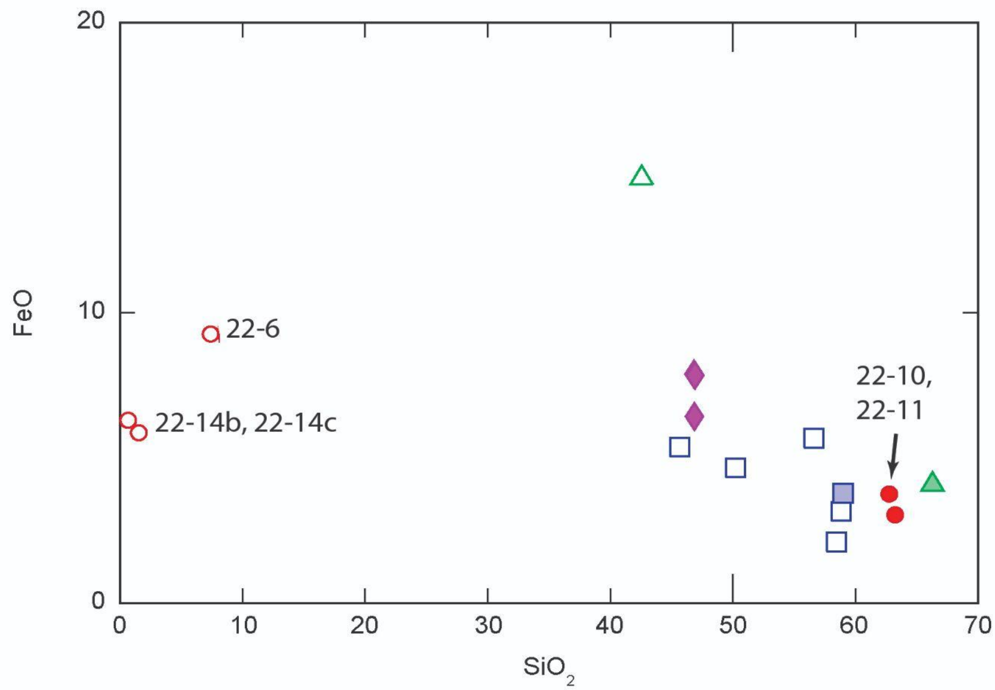

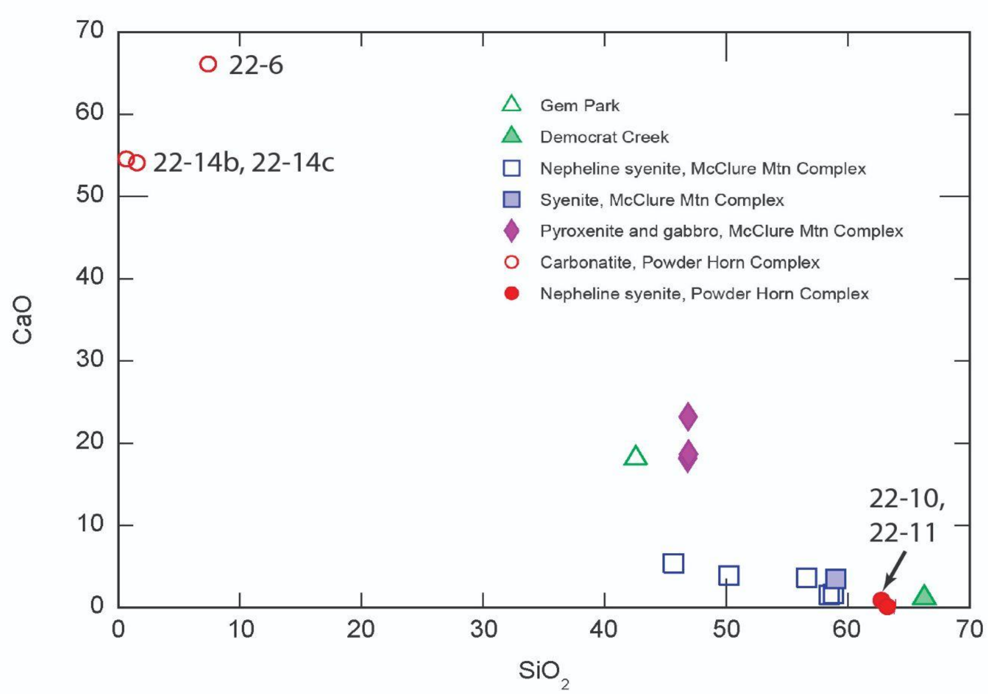

Fig. 39. (Upper Figure) FeO Harker variation diagram with oxides in weight percent.

Fig. 40. (Lower Figure) CaO Harker variation diagram with oxides in weight percent.

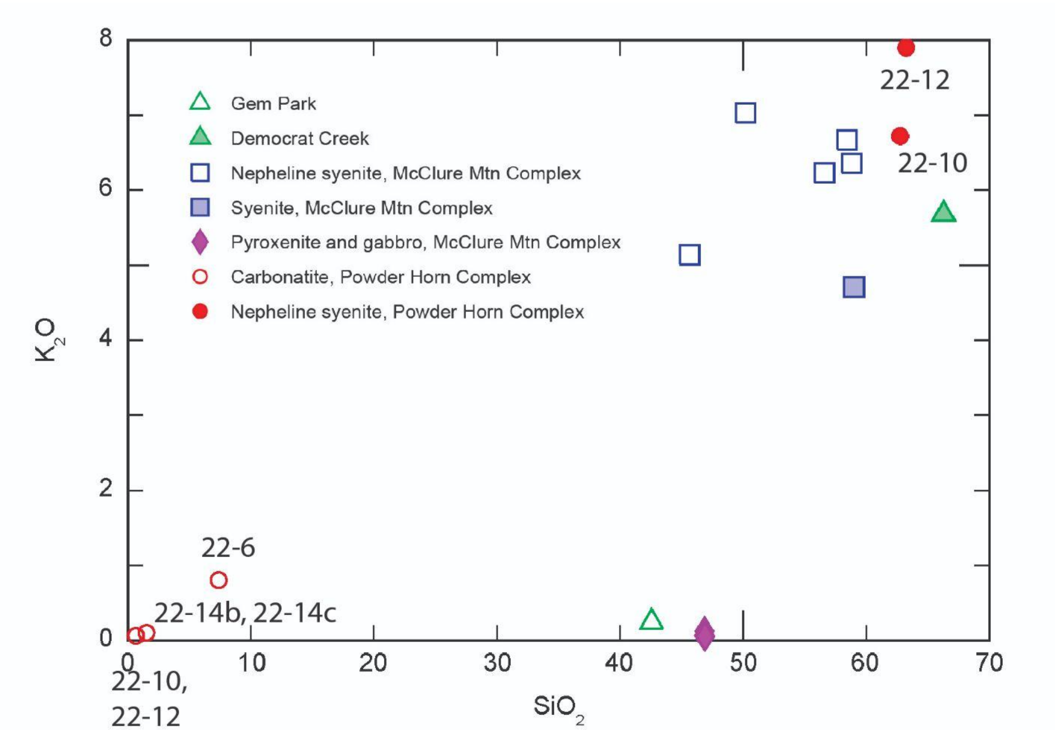

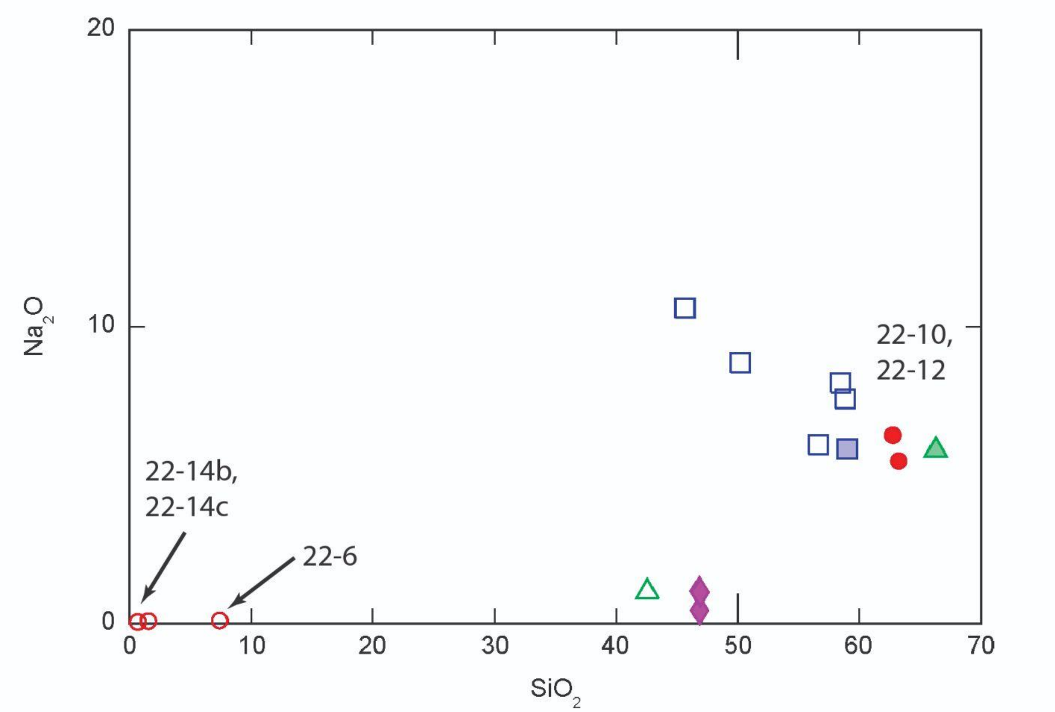

Fig. 41. (Upper Figure) K_2O Harker variation diagram with oxides in weight percent.

Fig. 42. (Lower Figure) Na_2O Harker variation diagram with oxides in weight percent.

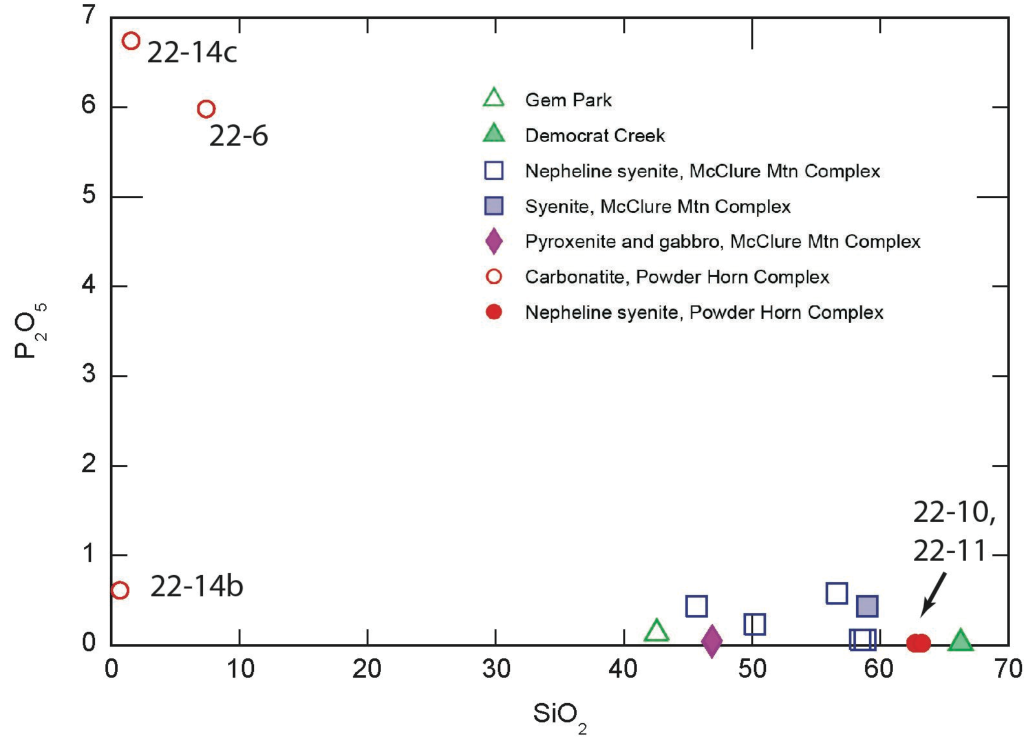

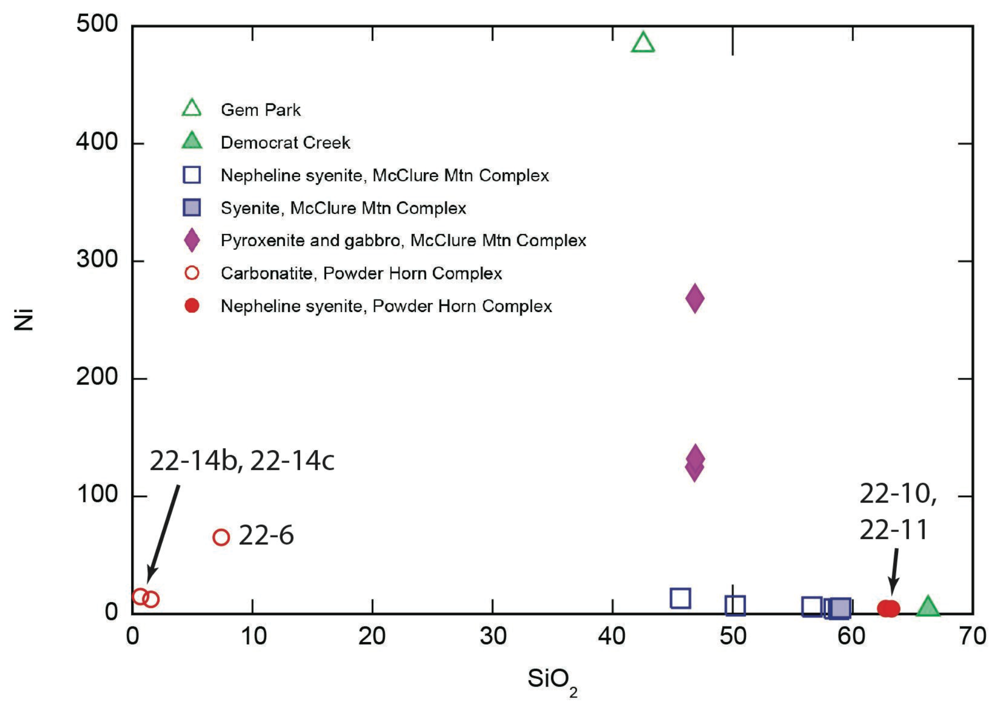

Fig. 43. (Upper Figure) P_2O_5 Harker variation diagram with oxides in weight percent.

Fig. 44. (Lower Figure) Ni Harker variation diagram with silica in weight percent and Ni in ppm.

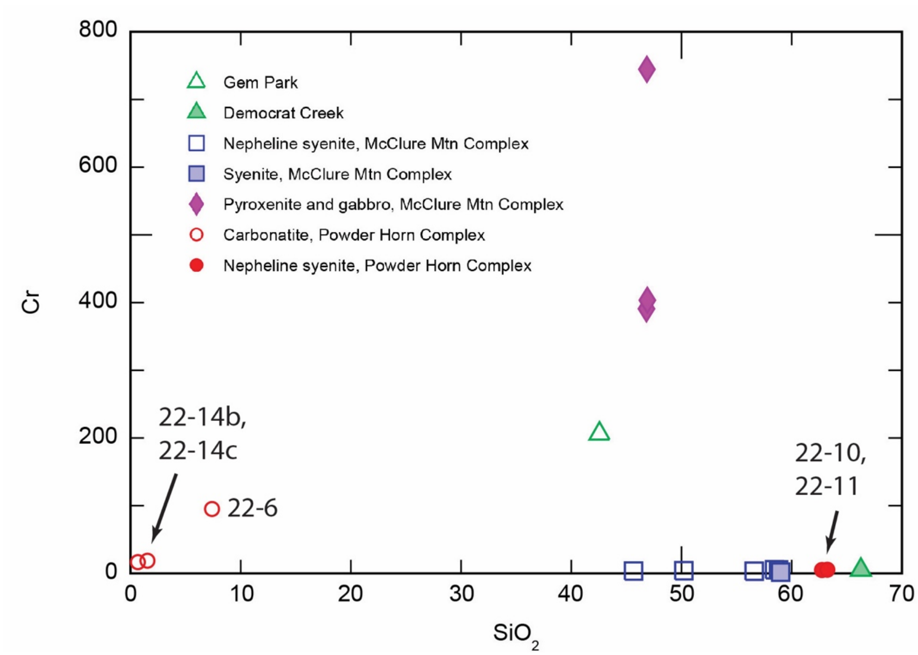

Fig. 45. Cr Harker variation diagram with silica in weight percent and Cr in ppm.

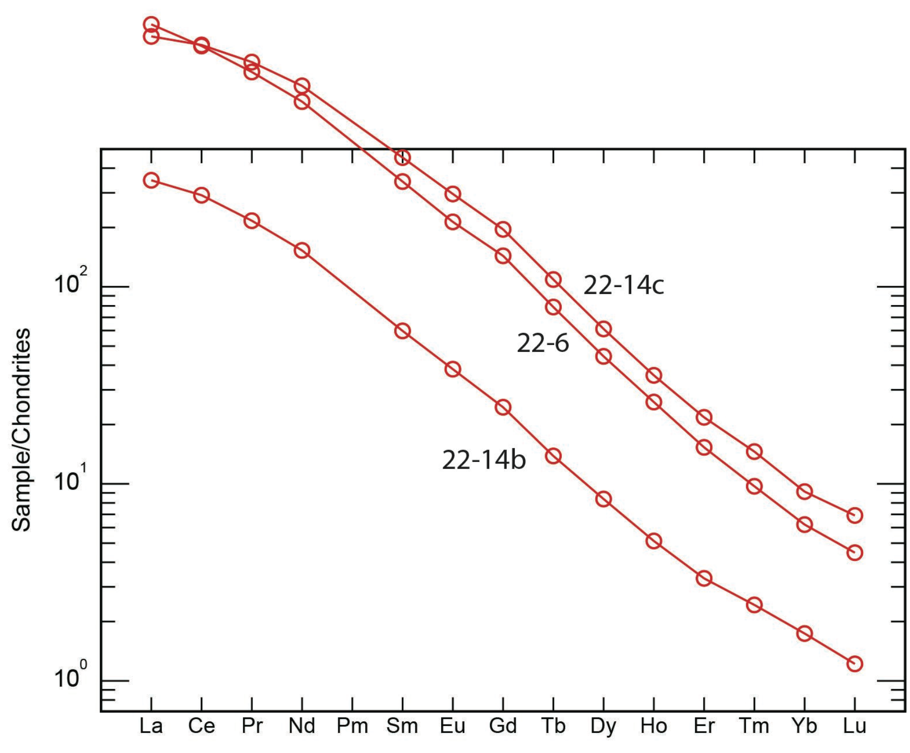

Fig. 46. REE element pattern for carbonatites in the Powderhorn Complex.

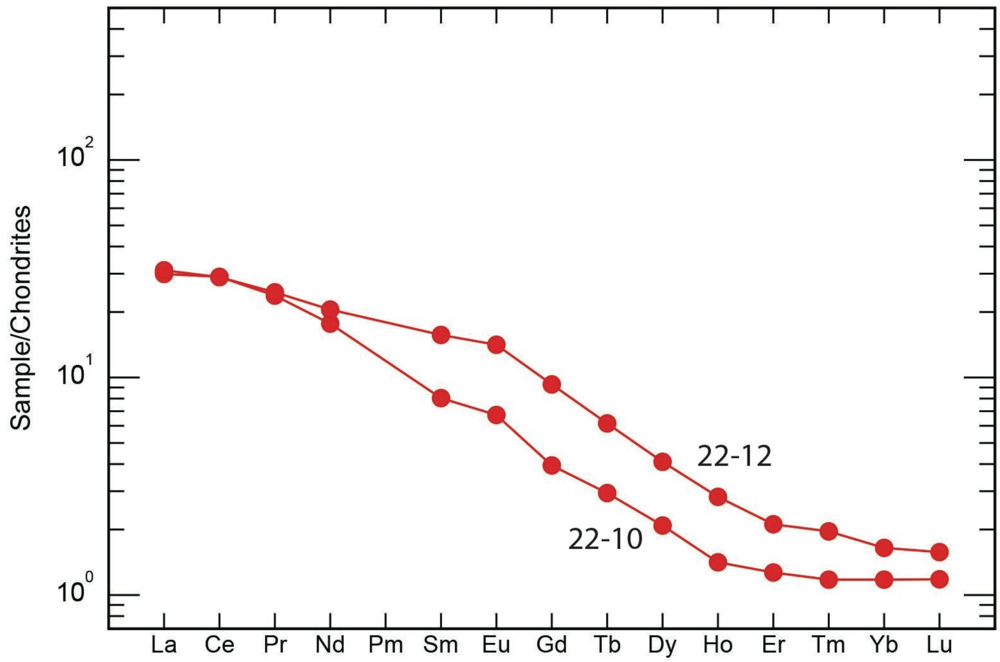

Fig. 47. REE element pattern for nepheline syenites in the Powderhorn Complex.

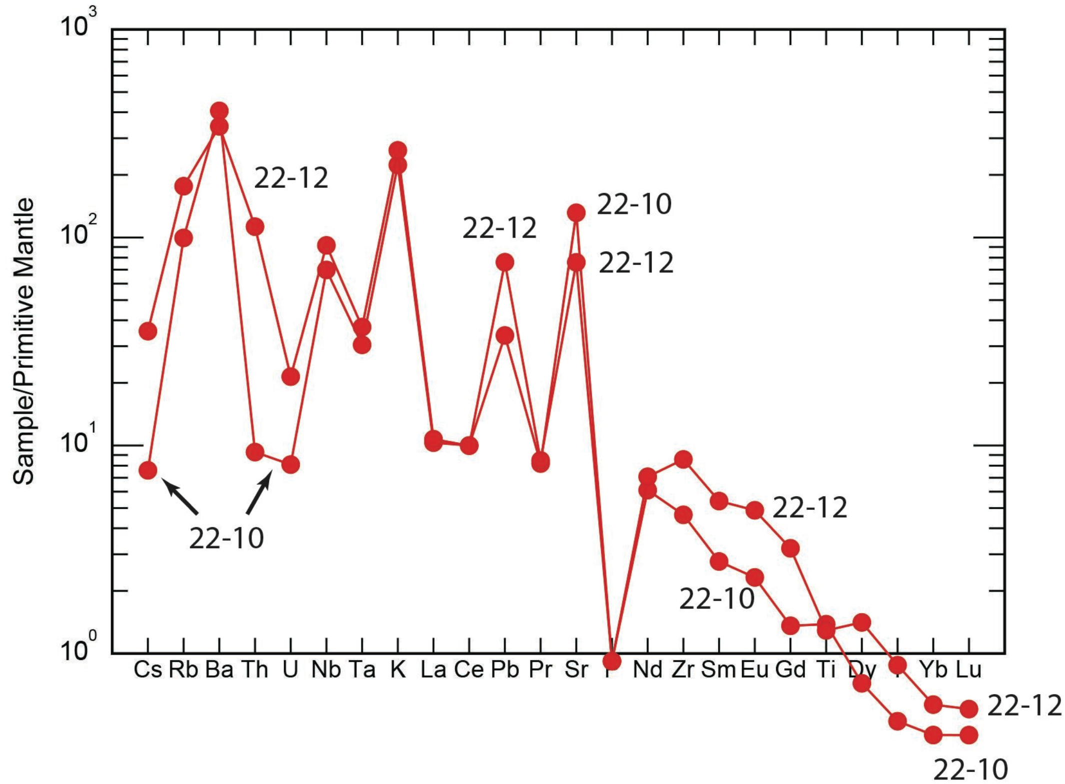

Fig. 48. Multi-element diagram for nepheline syenites in the Powderhorn Complex.

Conclusions

Cambrian to Ordovician plutonic igneous intrusions in parts of Colorado possibly related to the Southern Oklahoma rift include a variety of igneous rock types including pyroxenite, nepheline syenite, sodalite nepheline syenite, syenite, olivine gabbro, local quartz syenite, and a major carbonatite intrusion. Nepheline syenite and sodalite nepheline syenite represent silica-undersaturated magmas, meaning there is a deficiency of silica in the magma that forms nepheline and sodalite instead of the more typical sodium- and potassium-rich feldspars which can form in silica-saturated and oversaturated magmas. The only silica-oversaturated rocks we have collected consist of quartz syenite and come from the Democrat Creek Complex. This is in contrast to the Southern Oklahoma rift where there are large volumes of granite and the volcanic equivalent rhyolite, both of which are silica-oversaturated and contain abundant quartz. Therefore, the Cambrian to Ordovician igneous intrusions in Colorado must have formed by different processes than those in southern Oklahoma. The intrusions in Colorado also occur in much smaller volumes than the silica-oversaturated igneous rocks in southern Oklahoma, which is characteristic of carbonatites and nepheline-bearing igneous rocks worldwide. The intrusions in Colorado could represent a continuation of the rift from southern Oklahoma, but this needs to be confirmed by isotopic dating now in progress.

In the Wet Mountains, diopside-rich pyroxenite from the Gem Park Complex shows geochemical characteristics typical of cumulate rocks that settled on the floor of a magma chamber. In the McClure Mountain Complex, cumulate olivine gabbros and pyroxenite also occur and have typical geochemistry for cumulate rocks. However, the Gem Park Complex shows distinct differences in some of its major oxides and trace elements, meaning it represents a different batch of magma that intruded in a different area.

Nepheline syenite sample CO23-5 shows a very different REE pattern than the other nepheline syenites in the McClure Mountain Complex, which indicates that different small pulses of magma were injected into a limited area during the evolution of the complex. The Democrat Creek Complex contains relatively large volumes of silica-oversaturated quartz syenite which cannot be related to the nepheline syenites in the McClure Mountain Complex. The Democrat Creek sample CO22-5 shows strong negative Eu and Ba anomalies, indicating it is the result of prolonged fractional crystallization from a parental magma unrelated to the McClure Mountain Complex.

Nepheline syenites in the Powderhorn Complex are geochemically very similar and represent a single batch of magma. However, they show distinct differences in geochemistry from the nepheline syenites in the McClure Mountain Complex and must have had a somewhat different origin. There is a large compositional gap between the Powderhorn Complex carbonatites and the associated nepheline syenites. They must have formed from unrelated magmas. The distinct compositional differences between the three carbonatite samples analyzed indicate that the carbonatite formed from different smaller injections of magma in a similar manner to the McClure Mountain nepheline syenites.

References

Best, M. G., 2003. *Igneous and metamorphic petrology* Blackwell Publishing.

Gill, R., 2010. *Igneous rocks and processes: A practical guide*. Wiley-Blackwell.

Hanson, R., Puckett, R., Keller, G., Brueseke, M., Bulen, C., Mertzman, S., Finegan., S., McCleery, D.A., 2013. Intraplate magmatism related to the opening of the southern Iapetus Ocean: Cambrian Wichita igneous province in the Southern Oklahoma rift zone: *Lithos*, v. 174, p. 57-70.

Jones, A. P., Genge, M., Carmody, L., Hazen, R. M., Baross, J. A., 2013. Carbonate melts and carbonatites: *Reviews in Mineralogy and Geochemistry,* v. 75, p. 289-322.

Larson, E. E., Patterson, P. E., Curtis, G., Drake, R., Mutschler, F. E., 1985. Petrologic, paleomagnetic, and structural evidence of a Paleozoic rift system in Oklahoma, New Mexico, Colorado, and Utah: *Geological Society of America Bulletin*, v. 96, p. 1364-1372.

Magnin, B. P., Kuiper, Y. D., Anderson, E., 2023. Ediacaran-Ordovician magmatism and REE mineralization in the Wet Mountains, Colorado, USA; implications for failed continental rifting: *Tectonics,* v. 42, Article e2022TC007674.

Nesse, W. D. (2013). *Introduction to Optical Mineralogy.* Oxford Univ. Press.

Olson, J. C., Marvin, R. F., Parker, R. L., Mehnert, H. H., 1977. Age and tectonic setting of lower Paleozoic alkalic and mafic rocks, carbonatites, and thorium veins in south-central Colorado: *Journal of Research of the U. S. Geological Survey,* v. 5, p. 673-687.

Olson, J. C., Hedlund, D. C., 1981. Alkalic rocks and resources of thorium and associated elements in the Powderhorn district, Gunnison County, Colorado. *U.S. Geological Survey Professional Paper,* C1-C34.

Parker, R. L., Sharp, W. N., 1970. Mafic-ultramafic igneous rocks and associated carbonatites of the Gem Park Complex, Custer and Fremont Counties, Colorado. *U.S. Geological Survey Professional Paper,* 24.

Pivarunas, A. F., Meert, J., 2019. Protracted magmatism and magnetization around the McClure Mountain alkaline igneous complex: *Lithosphere,* v. 11, p. 590-602.

Rollinson, H. R., Pease, V., 2021. *Using geochemical data to understand geological processes:* Cambridge University Press.

Shawe, D. R., Parker, R. L., 1967. Mafic-ultramafic layered intrusion at Iron Mountain, Fremont County, Colorado: *U.S. Geological Survey Bulletin,* A1-A29.

Sun, S. S., McDonough, W. F., 1989. Chemical and isotopic systematics of oceanic basalts; implications for mantle composition and processes: *Geological Society Special Publications,* v. 42, p. 313-345.

Van Gosen, B., 2009. The Iron Hill (Powderhorn) carbonatite complex, Gunnison County, Colorado; a potential source of several uncommon mineral resources: *Open-File Report - U. S. Geological Survey,* 2009-1005, 28 p.

Wall, C., Hanson, R., Schmitz, M., Price, J., Donovan, R., Boro, J., Eschberger, A., Toews, C., 2021. Integrating zircon trace-element geochemistry and high-precision U-Pb zircon geochronology to resolve the timing and petrogenesis of the late Ediacaran-Cambrian Wichita igneous province, Southern Oklahoma aulacogen, USA: *Geology*, v. 49, p. 268-272.